

# Analysis of the Proteome of *Saccharomyces cerevisiae* for Methylarginine

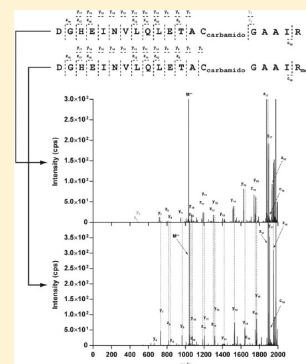
Jason K.K. Low, Gene Hart-Smith, Melissa A. Erce, and Marc R. Wilkins\*

Systems Biology Laboratory, School of Biotechnology and Biomolecular Sciences, The University of New South Wales, NSW 2052 Sydney, Australia

**S** Supporting Information

**ABSTRACT:** Arginine methylation is a post-translational modification that has been implicated in a plethora of cellular processes. In the present manuscript, using two antimethylarginine antibodies and combinatorial deletion mutants of arginine methyltransferases, we found evidence of widespread arginine methylation in the *Saccharomyces cerevisiae* proteome. Immunoprecipitation was used for enrichment of methylarginine-containing proteins, which were identified via tandem mass spectrometry. From this, we identified a total of 90 proteins, of which 5 were previously known to be methylated. The proteins identified were involved in known methylarginine-associated biological functions such as RNA processing, nuclear transport, carbohydrate metabolic process, GMP biosynthetic process and protein folding. Through in vivo methylation by the incorporation of [<sup>3</sup>H]-methyl groups, we validated the methylation of 7 proteins (Ded1, Imd4, Lhp1, Nop1, Cdc11, Gus1, Pob3). By LC–MS/MS, we then confirmed a total of 15 novel methylarginine sites on 5 proteins (Ded1, Lhp1, Nop1, Pab1, and Ugp1). By examination of methylation on proteins from the triple knockout of methyltransferases Hmt1, Hsl7, Rmt2, we present evidence for the existence of additional unidentified arginine methyltransferases in the *Saccharomyces cerevisiae* proteome.

**KEYWORDS:** arginine methylation, post-translational modification, *Saccharomyces cerevisiae*, methyltransferase

**■ INTRODUCTION**

Protein methylation has come under intense scrutiny and is now known to be of common occurrence. A recent report ranked methylation as the fourth most common post-translational modification (PTM).<sup>1</sup> In *Saccharomyces cerevisiae*, protein methylation has been reported to occur at the N- and C-terminus of polypeptides,<sup>2,3</sup> on glutamine,<sup>4</sup> histidine,<sup>5</sup> 2-(3-carboxy-3-aminopropyl)-L-histidine,<sup>6</sup> farnesyl-cysteine,<sup>7</sup> arginine,<sup>8,9</sup> lysine,<sup>10</sup> cysteine,<sup>11</sup> along with aspartic and glutamic acid residues.<sup>12</sup> The metabolic cost of methylation is high, 12 ATP molecules per methylation event.<sup>13</sup> This, together with the fact that multiple types of amino acid residues can be modified, suggests that methylation must play an important role in the cell.

Arginine methylation is conserved in eukaryotes and is not found in prokaryotes.<sup>14</sup> It has been shown to mediate protein–RNA, protein–DNA, and protein–protein interactions (for recent reviews see refs 15–17). Four different forms of methylarginines have been identified;  $\omega$ -N<sup>G</sup>,N<sup>G</sup>-asymmetric dimethylarginine (aDMA),  $\omega$ -N<sup>G</sup>,N<sup>G</sup>-symmetric dimethylarginine (sDMA),  $\omega$ -N<sup>G</sup>-monomethylarginine (MMA), and  $\delta$ -N-monomethylarginine ( $\delta$ -MMA). These methylation reactions are catalyzed by enzymes from the superfamily of S-adenosyl-L-methionine-(SAM)-dependent methyltransferases. To date, 3 protein arginine methyltransferases (Hmt1, Rmt2, and Sfm1) have been shown to be partly responsible for the aDMA, MMA, and  $\delta$ -MMA in *S. cerevisiae*. The last methyltransferase, Hsl7, has no known in vivo substrate (reviewed in ref 18). In total, 20 methylarginine-containing proteins have been described in *S. cerevisiae*, of which 15 are substrates of the major arginine methyltransferase, Hmt1.<sup>18</sup>

Methylation of arginine residues on *S. cerevisiae* proteins have been shown to be associated with several biological functions, including nucleocytoplasmic shuttling, RNA processing (mRNA and rRNA), and transcription (through histone and nonhistone proteins). Its involvement in other biological functions, such as splicing and translation are just beginning to be elucidated (reviewed in ref 18). In mammalian systems, arginine methylation has also been implicated in signal transduction and DNA repair (reviewed in ref 15). Methylarginine-containing proteins have also been found in the cytoskeleton,<sup>19</sup> Cajal bodies,<sup>20</sup> and Golgi apparatus,<sup>21</sup> although the exact function of this modification in these locations is currently unknown.

In the present manuscript, we utilized two commercially available, affinity-purified antimethylarginine antibodies to survey the degree of arginine methylation in *S. cerevisiae*. Although methylarginine-specific antibodies have been used previously to study methylarginine-containing proteins in yeast,<sup>22–24</sup> they have not been used to investigate the yeast proteome. In addition to immunoblot-based assays, we used one antibody to enrich for arginine-methylated proteins by immunoprecipitation. By use of tandem mass spectrometry (MS/MS), a total of 90 proteins were identified; these represent arginine methylated proteins and, will in some cases, also

Received: February 4, 2013

Published: July 18, 2013

represent their interaction partners. Five of the ninety were previously known to be arginine-methylated. The 90 proteins showed involvement in known methylarginine-associated biological functions such as RNA processing, nuclear transport, and translation. Interestingly, other proteins were of novel biological functions such as the carbohydrate metabolic process, protein folding, and the GMP biosynthetic process. By overexpression and purification, we successfully validated 9 of our putatively arginine-methylated proteins and identified a total of 15 novel methylarginine sites on 5 proteins. Through enzyme knockout analysis and the identification of methylarginine sites on 2 proteins purified from the triple arginine methyltransferase knockout mutant, we present evidence for the possibility of additional unidentified arginine methyltransferases in the *S. cerevisiae* proteome.

## METHODS

### Yeast Strains

*S. cerevisiae* BY4741 (*MATa his3Δ1 leu2Δ0 ura3Δ0 met15Δ0*) (#YSC1052, Open Biosystems) was used in this study. Yeasts were generally grown at 30 °C in YEPD media containing 2% (w/v) glucose, 2% (w/v) bactopectone, and 1% (w/v) yeast extract. For the growth and selection of yeast strains transformed with plasmids carrying the *URA3* marker, synthetic complete media without uracil (SC-ura) containing 2% (w/v) dextrose, 0.5% (w/v) ammonium sulfate, 0.17% (w/v) yeast nitrogen base (without ammonium sulfate) (#233520, BD Biosciences), and 0.192% (w/v) yeast synthetic drop-out medium supplement without uracil (#Y1501, Sigma-Aldrich) was used. Dextrose of choice was used as required; glucose for the maintenance and growth of strains and raffinose and galactose for the overexpression of proteins.

For the methyltransferase gene knockout analyses, single gene deletion strains were obtained from the *S. cerevisiae* Genome Deletion Project.<sup>25,26</sup> Unavailable single as well as double and triple gene deletions were generated using the PCR-based targeted gene deletion method<sup>27</sup> (see Methods of the Supporting Information). Transformation was performed using the lithium acetate-based method.<sup>28</sup>

### Immunoblots and Competitive Inhibition Immunoblots

Yeast cell extracts were prepared in lysis buffer (50 mM K-HEPES, 100 mM NaCl, 2 mM EDTA, 0.5% [v/v] Triton X-100, 2 mM DTT, protease inhibitors (#05892791001, Roche), adjusted to pH 7.5 with KOH) and lysed in a beadbeater (Biospec) using acid-washed glass beads (0.5 mm). Protein content was quantified using a modified Lowry assay (#500–0121, Biorad). Proteins were boiled in 1X SDS sample buffer (100 mM Tris-HCl pH 6.8, 5% [v/v] glycerol, 1.7% [w/v] SDS, 0.1 M DTT, and 0.002% [w/v] Bromophenol blue) for 5 min, resolved on a 4–12% NuPAGE Bis-Tris gel (Invitrogen) with MES–SDS PAGE buffer, and then electroblotted onto a PVDF membrane using standard methods. The rabbit antimonomethylarginine (anti-MMA) (#ICP0801, Immunechem) and rabbit antisymmetric dimethylarginine (anti-aDMA) (#ICP0810, Immunechem) antibodies were used at 1:1500 concentrations in the presence of 1% (w/v) BSA (#A3059, Sigma-Aldrich), and the secondary donkey antirabbit horse radish peroxidase-(HRP) conjugated antibody (#sc-2313, Santa Cruz Biotechnology) was used at a 1:5000 concentration in the presence of 0.8% (w/v) skim milk powder. Visualization of the immunoblots was achieved using a LAS3000 imager (Fujifilm). For competitive inhibition, 20 μg mL<sup>−1</sup> of free arginine (#A5006, Sigma-Aldrich),

free monomethylarginine (#M7033, Sigma-Aldrich), free asymmetrical dimethylarginine (#D4268, Sigma-Aldrich), or free symmetrical dimethylarginine (#D0390, Sigma-Aldrich) was added during the primary antibody incubation step.

### Immunoprecipitation

Anti-MMA antibodies were cross-linked to Dynabeads M-270 Epoxy (#143-21D, Invitrogen) as per the manufacturer's instructions. Antihemeagglutinin (HA) antibodies (#MMS-101P, Covance) were used as negative controls. Yeast cell extracts were prepared as described above with the exception of using the extraction buffer A, recommended by the manufacturer. For each immunoprecipitation reaction, lysate from ~0.250 g of wet cell paste was mixed with 4.5 mg of Dynabeads cross-linked with 22.5 μg of anti-MMA antibodies. The reactions were then incubated on a rotating wheel (4 °C, overnight), before the wash (4 × 900 μL, 2 min incubation, with extraction buffer A followed by 1 × 900 μL, 5 min incubation, with 1× last wash buffer with 0.02% Tween-20), and elution (3 × 60 μL, 5 min incubation, with supplied Elution Buffer) steps were performed. The eluates were then concentrated using an Amicon Ultra-0.5 mL Centrifugal Filter Unit (3000 MWCO, #42403, Millipore) to ~35 μL. Silver-staining of the SDS–PAGE-separated proteins was performed as described by Shevchenko et al.<sup>29</sup> For mass spectrometric analysis, visible gel bands and neighboring regions up to 3 mm were excised and prepared as described below.

### Overexpression and In vivo Methylation in *S. cerevisiae*

Overexpression plasmids were obtained from the Movable Open Reading Frame (MORF) library<sup>30</sup> (#YSC3868, Open Biosystems). Plasmids were verified by PCR and sequencing, using standard methods. Primers used can be found in Table S1 of the Supporting Information. Overexpression of proteins of interest was performed essentially as described by Gelperin et al. and Mok et al.<sup>30,31</sup> As a negative control, the plasmid pRS426<sup>32</sup> was used in place of a MORF plasmid. The tritium-based in vivo methylation of proteins in *S. cerevisiae* was adapted and modified from Xu et al.<sup>33</sup> Briefly, after the overexpression of proteins, 1.5 × 10<sup>7</sup> cells were harvested and resuspended in 82.8 μL of fresh overexpression media. Radiolabeling was then initiated by the addition of 8.6 μL of 7 μM SAM (#A7007, Sigma-Aldrich) and 8.6 μL of [<sup>3</sup>H]-SAM (4.7 μCi; #NET155H250UC, 81 Ci/mmol, PerkinElmer). Unlike Xu et al.,<sup>33</sup> no translational inhibitors were used. For reactions using less radiolabels, 15× less was used. The labeling reaction was allowed to continue for 90 min at 30 °C. The cells were then pelleted and incubated in 0.1 M NaOH for 5 min. After the removal of NaOH, lysis was achieved by adding 50 μL of hot 1× sample buffer and boiling for 10 min. Cell extracts were then separated on SDS–PAGE gels and electroblotted to PVDF, as above. To check for overexpression, the mouse antipentaHis-HRP conjugated antibodies (#34460, Qiagen) were used according to the manufacturer's instructions. For fluorography, the membranes were sprayed with EN<sup>3</sup>HANCE (#6NE970C, PerkinElmer) and the dried membranes were then exposed to preflashed film at −80 °C (#28-9068-42, GE healthcare). Dried films were then scanned in a Powerlook 1000 flatbed scanner (Umax) and saved as a TIFF file.

### Mass Spectrometry

Sample preparation and tandem mass spectrometry (MS/MS) methods for collision-induced dissociation (CID)-based and electron-transfer dissociation (ETD)-based MS/MS were performed as previously described.<sup>34</sup> Briefly, polyacrylamide

Table 1. Proteins Immunoprecipitated by the Anti-MMA Antibody and Identified by LC–MS/MS

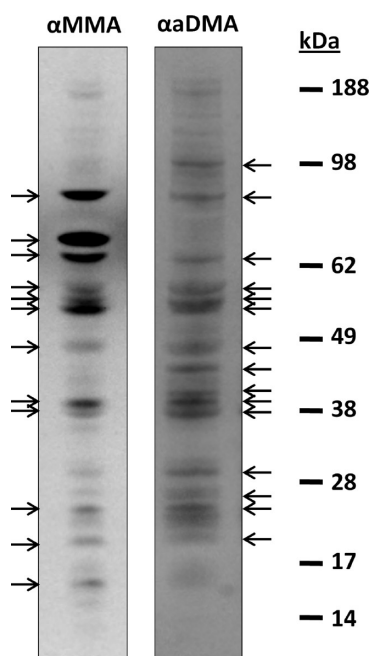
gene name <sup>a,b</sup>	name description	cellular location <sup>c,d</sup>	potential methyl-R sites <sup>e</sup>	mass score	unique peptide matches <sup>f</sup>
<b>wild-type</b>					
CDC33	eukaryotic translation initiation factor 4E	C, N	3	40	3 (1)
CPR6	peptidyl-prolylcis–trans isomerase CPR6	C	1	47	2 (1)
CRP1	cruciform DNA-recognizing protein 1	N, M	3	55	1 (1)
<b>DED1</b>	<b>ATP-dependent RNA helicase DED1</b>	<b>C</b>	<b>22</b>	<b>85</b>	<b>5 (3)</b>
<b>DYS1</b>	<b>deoxyhypusine synthase</b>	<b>C</b>	<b>7</b>	<b>63</b>	<b>2 (1)</b>
<b>ENO1</b>	<b>enolase 1</b>	<b>C, Mt</b>	<b>7</b>	<b>71</b>	<b>2 (1)</b>
<b>ENO2</b>	<b>enolase 2</b>	<b>C, M, Mt</b>	<b>6</b>	<b>129</b>	<b>3 (3)</b>
<b>HSC82 (HSP82)</b>	<b>ATP-dependent molecular chaperone HSC82</b>	<b>C, Mt</b>	<b>3</b>	<b>73</b>	<b>1 (1)</b>
<b>IMD4 (IMD3)</b>	<b>inosine-5'-monophosphate dehydrogenase 4</b>	<b>C</b>	<b>5</b>	<b>98</b>	<b>3 (2)</b>
<b>LHP1</b>	<b>La protein homologue</b>	<b>N, Nu</b>	<b>3</b>	<b>88</b>	<b>4 (3)</b>
<b>MAM33</b>	<b>mitochondrial acidic protein MAM33</b>	<b>C, Mt</b>	<b>1</b>	<b>58</b>	<b>1 (1)</b>
<b>MBF1</b>	<b>multiprotein-bridging factor 1</b>	<b>C, N, Mt</b>	<b>6</b>	<b>44</b>	<b>1 (1)</b>
<b>MRT4</b>	<b>mRNA turnover protein 4</b>	<b>N, Nu</b>	<b>2</b>	<b>45</b>	<b>4 (1)</b>
<b>NAP1</b>	<b>nucleosome assembly protein</b>	<b>C, N</b>	<b>3</b>	<b>38</b>	<b>1 (1)</b>
<b>NHP6A</b>	<b>nonhistone chromosomal protein 6A</b>	<b>N</b>	<b>0</b>	<b>43</b>	<b>2 (1)</b>
<b>NHP6B</b>	<b>nonhistone chromosomal protein 6B</b>	<b>N</b>	<b>1</b>	<b>68</b>	<b>1 (1)</b>
<b>NOP1*</b>	<b>rRNA 2'-O-methyltransferase fibrillarin</b>	<b>C, N, Nu</b>	<b>22</b>	<b>257</b>	<b>5 (4)</b>
<b>NOP6</b>	<b>nucleolar protein 6</b>	<b>N, Nu</b>	<b>4</b>	<b>95</b>	<b>4 (3)</b>
<b>NSR1*</b>	<b>nuclear localization sequence-binding protein</b>	<b>C, N, Nu, Mt</b>	<b>13</b>	<b>52</b>	<b>2 (2)</b>
<b>PAB1</b>	<b>poly(A)-binding protein</b>	<b>C, N</b>	<b>3</b>	<b>101</b>	<b>5 (2)</b>
<b>PGK1</b>	<b>phosphoglycerate kinase</b>	<b>C, N, Mt</b>	<b>0</b>	<b>72</b>	<b>1 (1)</b>
<b>PRT1</b>	<b>eukaryotic translation initiation factor 3 subunit B</b>	<b>C</b>	<b>7</b>	<b>48</b>	<b>1 (1)</b>
<b>PWP1</b>	<b>periodic tryptophan protein 1</b>	<b>C, N, Nu</b>	<b>4</b>	<b>42</b>	<b>1 (1)</b>
<b>RIM1</b>	<b>mitochondrial ssDNA-binding protein</b>	<b>C, Mt</b>	<b>3</b>	<b>46</b>	<b>1 (1)</b>
<b>RPL11A</b>	<b>60 S ribosomal protein L11-A</b>	<b>C</b>	<b>6</b>	<b>69</b>	<b>4 (2)</b>
<b>RPL13A (RPL13B)</b>	<b>60 S ribosomal protein L13-A</b>	<b>C</b>	<b>5</b>	<b>61</b>	<b>2 (2)</b>
<b>RPL22A</b>	<b>60 S ribosomal protein L22-A</b>	<b>C</b>	<b>0</b>	<b>134</b>	<b>3 (3)</b>
<b>RPL22B</b>	<b>60 S ribosomal protein L22-B</b>	<b>C</b>	<b>0</b>	<b>59</b>	<b>1 (1)</b>
<b>RPL26A (RPL26B)</b>	<b>60 S ribosomal protein L26-A</b>	<b>C</b>	<b>2</b>	<b>47</b>	<b>2 (1)</b>
<b>RPL30</b>	<b>60 S ribosomal protein L30</b>	<b>C</b>	<b>2</b>	<b>163</b>	<b>6 (3)</b>
<b>RPL31A (RPL31B)</b>	<b>60 S ribosomal protein L31-A</b>	<b>C</b>	<b>4</b>	<b>55</b>	<b>3 (2)</b>
<b>RPL38</b>	<b>60 S ribosomal protein L38</b>	<b>C</b>	<b>1</b>	<b>47</b>	<b>1 (1)</b>
<b>RPL5</b>	<b>60 S ribosomal protein L5</b>	<b>C</b>	<b>6</b>	<b>102</b>	<b>2 (2)</b>
<b>RPL6B (RPL6A)</b>	<b>60 S ribosomal protein L6-B</b>	<b>C</b>	<b>2</b>	<b>167</b>	<b>6 (2)</b>
<b>RPL8B (RPL8A)</b>	<b>60 S ribosomal protein L8-B</b>	<b>C</b>	<b>2</b>	<b>208</b>	<b>11 (9)</b>
<b>RPP0</b>	<b>60 S acidic ribosomal protein P0</b>	<b>C</b>	<b>6</b>	<b>135</b>	<b>5 (4)</b>
<b>RPP1B</b>	<b>60 S acidic ribosomal protein P1-beta</b>	<b>C</b>	<b>0</b>	<b>100</b>	<b>1 (1)</b>
<b>RPP2B</b>	<b>60 S acidic ribosomal protein P2-beta</b>	<b>C</b>	<b>0</b>	<b>87</b>	<b>3 (3)</b>
<b>RPS19A (RPS19B)</b>	<b>40 S ribosomal protein S19-A</b>	<b>C</b>	<b>3</b>	<b>85</b>	<b>2 (2)</b>
<b>RPS22A (RPS22B)</b>	<b>40 S ribosomal protein S22-A</b>	<b>C, N, Nu</b>	<b>1</b>	<b>170</b>	<b>2 (2)</b>
<b>RPS28A (RPS28B)</b>	<b>40 S ribosomal protein S28-A</b>	<b>C</b>	<b>4</b>	<b>45</b>	<b>2 (1)</b>
<b>RPS5</b>	<b>40 S ribosomal protein S5</b>	<b>C</b>	<b>3</b>	<b>108</b>	<b>2 (2)</b>
<b>RPS7A</b>	<b>40 S ribosomal protein S7-A</b>	<b>C</b>	<b>3</b>	<b>55</b>	<b>2 (1)</b>
<b>RRB1</b>	<b>ribosome assembly protein RRB1</b>	<b>N, Nu</b>	<b>2</b>	<b>115</b>	<b>3 (3)</b>
<b>RRP5</b>	<b>rRNA biogenesis protein RRP5</b>	<b>N, Nu</b>	<b>14</b>	<b>57</b>	<b>1 (1)</b>
<b>SBP1*</b>	<b>single-stranded nucleic acid-binding protein</b>	<b>C, N, Nu</b>	<b>16</b>	<b>58</b>	<b>1 (1)</b>
<b>SHM1</b>	<b>serine hydroxymethyltransferase, mitochondrial</b>	<b>C, Mt</b>	<b>8</b>	<b>169</b>	<b>4 (4)</b>
<b>SSB1</b>	<b>heat shock protein SSB1</b>	<b>C, M</b>	<b>6</b>	<b>501</b>	<b>22 (13)</b>
<b>SSB2</b>	<b>heat shock protein SSB2</b>	<b>C, M</b>	<b>6</b>	<b>484</b>	<b>22 (13)</b>
<b>SSC1</b>	<b>heat shock protein SSC1, mitochondrial</b>	<b>C, M, Mt</b>	<b>3</b>	<b>82</b>	<b>1 (1)</b>
<b>SSE1</b>	<b>heat shock protein homologue SSE1</b>	<b>C</b>	<b>8</b>	<b>43</b>	<b>1 (1)</b>
<b>TIF34</b>	<b>eukaryotic translation initiation factor 3 subunit I</b>	<b>C</b>	<b>4</b>	<b>43</b>	<b>1 (1)</b>
<b>TIM9</b>	<b>mitochondrial import inner membrane translocase subunit TIM9</b>	<b>C, M, Mt</b>	<b>1</b>	<b>83</b>	<b>2 (2)</b>
<b>YKL107W</b>	<b>uncharacterised oxidoreductase YKL107W</b>	<b>Unknown</b>	<b>5</b>	<b>48</b>	<b>1 (1)</b>
<b>YRA1*</b>	<b>RNA annealing protein YRA1</b>	<b>N</b>	<b>14</b>	<b>53</b>	<b>2 (1)</b>

Table 1. continued

gene name <sup>a,b</sup>	name description	cellular location <sup>c,d</sup>	potential methyl-R sites <sup>e</sup>	mascot score	unique peptide matches <sup>f</sup>
<b>Arginine methyltransferase triple knockout mutant</b>					
<i>ARC1</i>	GU4 nucleic-binding protein 1	C	3	151	5 (5)
<i>CBF5</i>	H/ACA ribonucleoprotein complex subunit 4	N, Nu	7	201	8 (7)
<i>CDC10</i>	cell division control protein 10	C, M	5	138	6 (3)
<i>CDC11</i>	cell division control protein 11	C, M	7	65	3 (1)
<i>CDC12</i>	cell division control protein 12	C, M	4	664	15 (10)
<i>CDC3</i>	cell division control protein 3	C, M	3	387	24 (12)
<i>DBP6</i>	ATP-dependent RNA helicase DBP6	N, Nu	7	73	2 (1)
<i>DED1</i>	ATP-dependent RNA helicase DED1	C	22	169	7 (5)
<i>DUR1,2</i>	urea amidolyase	C	21	64	1 (1)
<i>ENO2</i>	enolase 2	C, M, Mt, V	6	116	2 (2)
<i>ENT5</i>	epsin-5	C, M, G	5	43	1 (1)
<i>GUS1</i>	glutamate-tRNA ligase, cytoplasmic	C, Mt	14	100	4 (2)
<i>HAS1</i>	ATP-dependent RNA helicase HAS1	N, Nu	10	232	14 (7)
<i>IDP1</i>	oxalosuccinate decarboxylase	C, Mt	3	69	2 (1)
<i>IMD3 (IMD4)</i>	inosine-5'-monophosphate dehydrogenase 3	C, M	7	345	9 (6)
<i>KGD2</i>	2-oxoglutarate dehydrogenase complex component E2	C, Mt	3	45	1 (1)
<i>LAT1</i>	pyruvate dehydrogenase complex component E2	C, Mt	3	434	20 (12)
<i>LPD1</i>	pyruvate dehydrogenase complex E3 component	C, Mt	6	897	39 (24)
<i>MDH3</i>	malate dehydrogenase, peroxisomal	C, N, P	3	76	3 (2)
<i>NDI1</i>	NADH:ubiquinonereductase	C, Mt	5	49	2 (1)
<i>NOP1*</i>	rRNA 2'-O-methyltransferase fibrillarin	C, N, Nu	22	91	9 (2)
<i>NOP56</i>	nucleolar protein 56	N, Nu	1	45	1 (1)
<i>NSR1*</i>	nuclear localization sequence-binding protein	C, N, Nu, Mt	13	62	2 (2)
<i>PAB1</i>	poly(A)-binding protein	C, N	3	102	4 (3)
<i>PDA1</i>	pyruvate dehydrogenase E1 component subunit alpha, mitochondrial	C, Mt	11	486	26 (12)
<i>PDB1</i>	pyruvate dehydrogenase E1 component subunit beta, mitochondrial	C, Mt	5	541	19 (15)
<i>PIL1</i>	sphingolipid long chain base-responsive protein PIL1	C, Mt, M, PC	3	51	1 (1)
<i>POB3</i>	FACT complex subunit POB3	N	11	76	1 (1)
<i>PYC1 (PYC2)</i>	pyruvate carboxylase 1	C	13	129	3 (2)
<i>REAI</i>	replication factor A protein 1	C, N	10	388	21 (10)
<i>RPL13A (RPL13B)</i>	60 S ribosomal protein L13-A	C	5	43	2 (1)
<i>RPL30</i>	60 S ribosomal protein L30	C	2	88	3 (2)
<i>RPL7A (RPL7B)</i>	60 S ribosomal protein L7-A	C	2	45	1 (1)
<i>RPL8B (RPL8A)</i>	60 S ribosomal protein L8-B	C	2	45	1 (1)
<i>RPP2B</i>	60 S acidic ribosomal protein P2-beta	C	0	60	1 (1)
<i>RPS14A (RPS14B)</i>	40 S ribosomal protein S14-A	C	6	47	2 (1)
<i>RPS19A</i>	40 S ribosomal protein S19-A	C	3	48	1 (1)
<i>RPS3*</i>	40 S ribosomal protein S3	C	5	56	1 (1)
<i>RPS7A</i>	40 S ribosomal protein S7-A	C	3	53	1 (1)
<i>RRB1</i>	ribosome assembly protein RRB1	N, Nu	2	201	8 (5)
<i>RRP9</i>	ribosomal RNA-processing protein 9	N, Nu	12	70	4 (2)
<i>SES1</i>	serine-tRNA ligase, cytoplasmic	C	5	68	1 (1)
<i>SRP40</i>	suppressor protein SRP40	N, Nu	5	44	2 (1)
<i>SSB1</i>	heat shock protein SSB1	C, M	6	515	18 (12)
<i>SSB2</i>	heat shock protein SSB2	C, M	6	546	17 (11)
<i>TIM9</i>	mitochondrial import inner membrane translocase subunit TIM9	C, M, Mt	1	80	2 (1)
<i>UGP1</i>	UTP-glucose-1-phosphate uridylyltransferase	C, M	8	697	31 (17)
<i>UTP15</i>	U3 snoRNA-associated protein 15	N, Nu	9	43	3 (1)
<i>YTM1</i>	ribosome biogenesis protein YTM1	N, Nu	11	83	4 (2)
<i>gag</i>	yeast L-A totivirus major capsid protein	—	8	560	16 (6)

<sup>a</sup>Known methylarginine substrates are marked with an asterisk (\*). <sup>b</sup>Proteins in parentheses are found within a cluster of homologous proteins and cannot be confidently distinguished from its homologue. Note that they may not share all identified peptides with its homologue (For peptide details, see Table S5 of the Supporting Information and for data analysis details, see Methods). <sup>c</sup>Legend: C, cytoplasm; N, nucleus; Nu, nucleolus; M, membrane; Mt, mitochondrion; V, vacuole; G, Golgi apparatus; P, peroxisome; and PC, punctate composite. <sup>d</sup>Where available, localization data were sourced from the SGD <sup>38</sup> and from Huh et al. <sup>40</sup> <sup>e</sup>The RXG and RGX motifs are from Wooderchak et al. (2008); <sup>41</sup> GXXR and WXXR motifs are from Pang et al. (2010); <sup>42</sup> RXR motif is from Smith et al. <sup>43</sup> Proteins with 5 or more sites are in bold. <sup>f</sup>Number of unique peptides identified during MS/MS for each protein. Number of peptide(s) with Mascot scores  $\geq 37$  are in parentheses.





**Figure 1.** Extensive arginine methylation is present in the *S. cerevisiae* proteome. One-dimensional SDS–PAGE separations of wild-type yeast cell extracts were blotted to PVDF and probed with either anti-MMA ( $\alpha$ MMA) or anti-aDMA ( $\alpha$ aDMA) antibodies. Major bands detected are denoted by arrows. From both antibodies, we observed a total of 55 methylated protein candidates in a wide range of molecular weights. Of these, 12 and 15 bands (as arrowed) were identified as major bands in the anti-MMA and anti-aDMA blots, respectively. The remaining bands were detected at lesser intensities and were, hence, considered as minor bands (not indicated).

gel samples were destained, reduced, and alkylated following the procedure described by Shevchenko et al.<sup>29</sup> For protein digestion, 4 ng of trypsin (#V5111, Promega) in 40  $\mu$ L of 0.1 M  $\text{NH}_4\text{HCO}_3$  was used and incubation was for 16 h at 35  $^\circ\text{C}$ . The digest solutions were removed to new microfuge tubes and the gel slices were treated with each of the following solutions sequentially for 30 min each: 50  $\mu$ L 0.1% (v/v) trifluoroacetic acid (TFA), 50  $\mu$ L 0.1% (v/v) TFA/60% (v/v) acetonitrile (ACN), and 50  $\mu$ L 100% ACN. The pooled digest and peptide extraction solutions were then dried (Savant SPD1010, Thermo-fisher Scientific) before resuspending in 20  $\mu$ L of 1% (v/v) formic acid and 0.05% (v/v) heptafluorobutyric acid (HFBA).

Digested peptide samples were separated by nanoliquid chromatography (LC) using an Ultimate 3000 HPLC and autosampler system (Dionex). Samples were concentrated and desalted onto a micro C18 precolumn (500  $\mu\text{m} \times 2$  mm, Michrom Bioresources) with  $\text{H}_2\text{O}:\text{CH}_3\text{CN}$  [98:2, 0.05% (v/v) HFBA] at 20  $\mu\text{L min}^{-1}$ . After a 4 min wash, the precolumn was switched (Valco 10 port valve, Dionex) into line with a fritless nano column (75  $\mu\text{m} \times \sim 10$  cm) containing C18 media (5  $\mu\text{m}$ , 200  $\text{\AA}$  Magic, Michrom) manufactured according to Gatlin et al.<sup>35</sup> Peptides were eluted using a linear gradient of  $\text{H}_2\text{O}:\text{CH}_3\text{CN}$  [98:2, 0.1% (v/v) formic acid] to  $\text{H}_2\text{O}:\text{CH}_3\text{CN}$  [64:36, 0.1% (v/v) formic acid] at 350 nL  $\text{min}^{-1}$  over 30 min. High voltage (1800 V) was applied to a low volume tee (Upchurch Scientific) and the column tip positioned  $\sim 0.5$  cm from the heated capillary (250  $^\circ\text{C}$ ) of the mass spectrometer. Positive ions were generated by electrospray.

For CID MS/MS following LC and electrospray, either an LTQ FT Ultra mass spectrometer (Thermo Electron) or an

LTQ Orbitrap Velos (Thermo Electron) hybrid linear ion trap mass spectrometer was used. Data-dependent acquisition (DDA) was used at all times unless otherwise stated. For the LTQ FT Ultra, survey scans of  $m/z$  350–1750 were acquired in the FT ICR cell (resolution =  $1 \times 10^5$  at  $m/z$  400, with an accumulation target value of  $1 \times 10^6$  ions). Up to the 6 most abundant ions ( $>3000$  counts) with charge states  $\geq +2$  were sequentially isolated and fragmented within the linear ion trap using CID with an activation  $q = 0.25$  and activation time of 30 ms at a target value of 30000 ions. Selected  $m/z$  values for MS/MS were dynamically excluded for 30 s. For the LTQ Orbitrap Velos, survey scans  $m/z$  350–2000 were acquired in the Orbitrap (resolution 30000 at  $m/z$  400, with an accumulation target value of  $1 \times 10^6$  ions). Up to the 10 most abundant ions ( $>5000$  counts) with charge states  $\geq +2$  were sequentially isolated and fragmented within the linear ion trap using CID with an activation  $q = 0.25$ , an activation time of 30 ms, normalized collision energy of 30%, and a target value of 10000 ions. Precursor ion widths of 2.0 were used, and  $m/z$  values selected for MS/MS were dynamically excluded for 45 s. Peak lists were generated using Mascot Daemon/extract\_msn (version 2.3, Matrix Science) using default parameters.

For ETD MS/MS, the LTQ Orbitrap Velos (Thermo Electron) hybrid linear ion trap mass spectrometer was used; the methods used for LC, electrospray and survey scans were identical to those employed during CID-based LC–MS/MS. ETD was performed with a target value of 10000 ions, a 130 ms reaction time, and with supplemental activation employed; target values for fluoranthene anions ranged from  $7 \times 10^5$  to  $4 \times 10^6$ .

Peak lists derived from LC–MS/MS were submitted to the database search program Mascot (version 2.3, Matrix Science).<sup>36</sup> The following search parameters were employed: instrument type was ESI-TRAP or ETD-TRAP for CID- and ETD-derived data, respectively; peptide and peptide fragment mass tolerances were  $\pm 4$  ppm and  $\pm 0.4$  Da, respectively; standard variable modifications included were acrylamide (C), carbamidomethyl (C), and oxidation (M), additional variable modifications for the various post-translation modifications were included when required [e.g., methylarginine (R) and dimethylarginine (R)], and enzyme specificity was trypsin with up to 3 missed cleavages and all taxonomies in the Swiss-Prot database (July 2012 release, 536789 sequence entries) were searched.

Proteins identified from MS/MS were manually filtered to only include protein identifications with at least one peptide with a Mascot ion score  $\geq 37$  and expect-values ( $E$ -values)  $< 0.05$ . All identified proteins had to be statistically significant ( $p < 0.05$ ) according to the Mascot expect metric. For post-translationally modified peptides identified via Mascot, fragment-ion series were manually inspected to confirm unambiguous localizations of modification sites, and the observations of methylarginine-associated neutral losses from charge-reduced precursor ions were used to further support modified peptide characterisations.<sup>37</sup> Proteins with single peptide identifications were also individually inspected (Figures S20–S51 of the Supporting Information). Proteins that were identified in the negative control immunoprecipitations were treated as nonspecific background and were removed from the list of wild type and knockout mutant-derived proteins. Proteins found within homologous protein clusters that share all MS/MS-identified peptides cannot be distinguished separately by Mascot database searching. All protein clusters were included in Table 1. However, during subsequent data analysis, protein clusters were considered as a single protein entry.

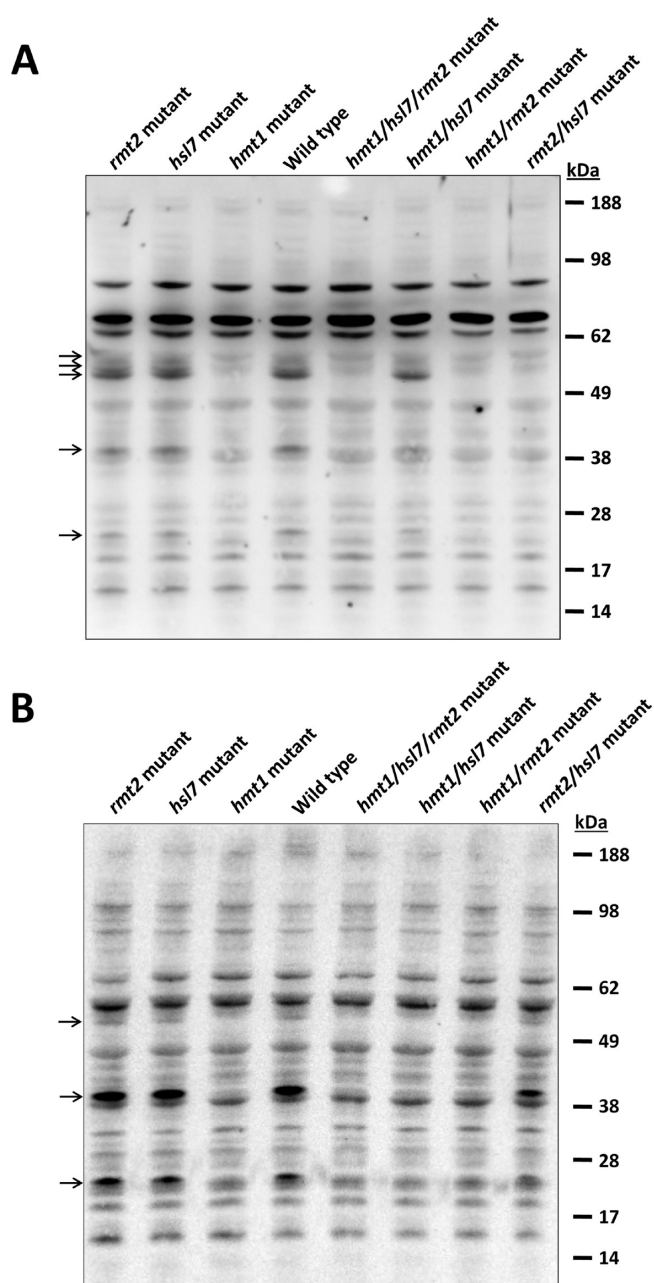


**Figure 2.** Arginine methylation is present in the triple methyltransferase knockout mutant. One-dimensional SDS–PAGE separations of arginine methyltransferase gene deletion mutants were blotted to PVDF and probed with antimethylarginine antibodies. These antibodies detected differences in methylation states in the different arginine methyltransferase mutants. All differences observed were due to the deletion of the *HMT1* gene. Interestingly, methylarginines are still detected in the triple gene (*hmt1/hsl7/rmt2*) knockout mutant. Selected differences observed in methylation are denoted by arrows on the left of the blots. Protein-stained images to show amount of protein loading are in Figure S4 of the Supporting Information. (A) *S. cerevisiae* cell extracts probed with the anti-MMA antibody. Some differences that were observed included the major bands denoted by arrows on the left. (B) *S. cerevisiae* cell extracts probed with the anti-aDMA antibody. Some differences that were observed included the major bands denoted by arrows on the left.

### Data Analysis

Biological process and molecular function gene ontology (GO) terms were sourced from the *Saccharomyces* Genome Database

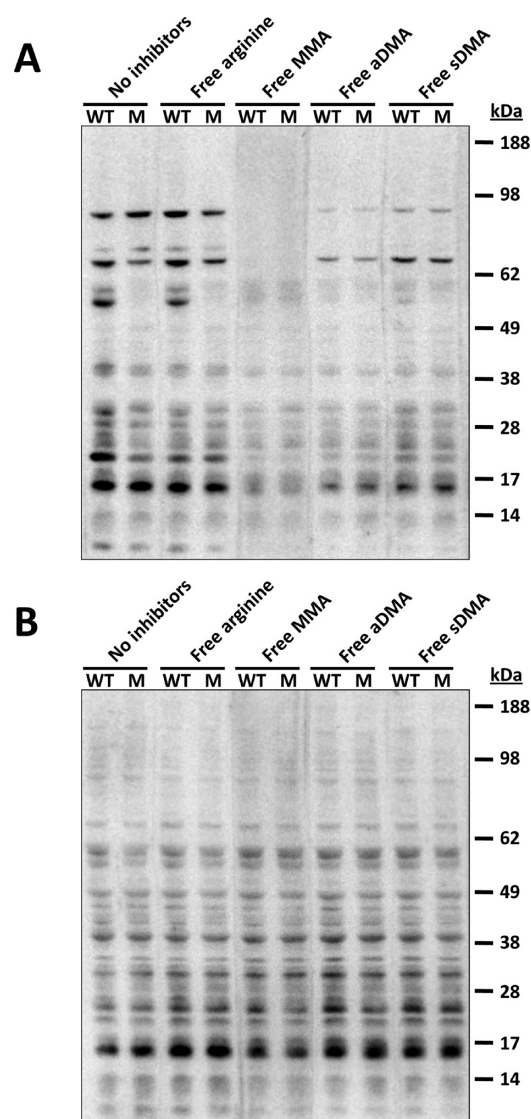


**Figure 3.** Competitive inhibition shows that the anti-MMA antibodies are specific, while the anti-aDMA antibodies are not. One-dimensional SDS–PAGE separations of *S. cerevisiae* wild-type (WT) and arginine methyltransferase triple knockout mutant (M) cell extracts were blotted to PVDF and probed with antimethylarginine antibodies. During primary antibody incubation, either free unmodified or modified arginines were added as competitive inhibitors. Protein-stained images to show amount of protein loading are in Figure S5 of the Supporting Information. (A) Immunoblots were probed with anti-MMA antibody. In the presence of free MMA, the anti-MMA antibody was strongly inhibited. Reduced inhibition was observed in the presence of free aDMA or sDMA, with sDMA showing the least inhibitory effect. Importantly, no inhibition was observed with free unmodified arginines. These results suggest that the anti-MMA antibody is specific to methylarginines with the highest affinity to monomethylarginines. (B) Immunoblots were probed with anti-aDMA antibody. In contrast to the anti-MMA antibody, no significant inhibition was observed in the presence of both unmodified and modified arginines. These results suggest that the anti-aDMA antibody is not specific to methylarginines.

(SGD) GO slim mapper tool<sup>38</sup> and from the Uniprot Consortium.<sup>39</sup> Cellular localization data were sourced from SGD<sup>38</sup> and from Huh et al.<sup>40</sup> Potential methylation sites were identified by manually examining primary sequences for the presence of arginine methylation motifs. Motifs included in the search were the RXG and RGX motifs from Wooderchak et al.,<sup>41</sup> GXXR and

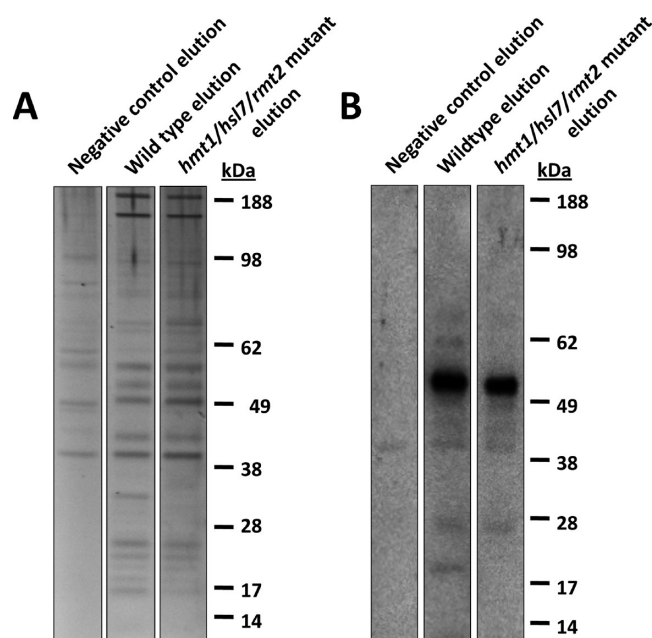


**Figure 4.** Immunoprecipitation for the enrichment of methylarginine-containing proteins. Immunoprecipitation of the wild-type and the arginine methyltransferase triple knockout mutant strains were performed using the anti-MMA antibodies. As a negative control, anti-HA antibodies were used. (A) Immunoprecipitates were analyzed via SDS-PAGE and silver staining. Key similarities between the wild-type (lane 2) and the triple knockout mutant (lane 3) were the protein bands in the region between 40 and 70 kDa and in the 16 to 25 kDa region. Whereas, key differences observed were that there were more bands with differing intensities observed in the wild-type immunoprecipitates, such as the 35 and 17 kDa regions. Several bands were present in the negative control (lane 1). However, most of these bands do not correspond to those seen in the wild-type or mutant lanes (lanes 2 and 3). When compared to the immunoblots (Figure 1), it is notable that several major protein bands observed in Figure 1 at 63, 57, 53, 24, 20, and 16 kDa were also present in the immunoprecipitates shown in this figure. Additional major bands seen only in the immunoprecipitates were observed at 160, 49, 43, 41, and 35 kDa. (B) Corresponding immunoblot using the same anti-MMA antibody against the same set of immunoprecipitated proteins shown in panel A shows modest enrichment of arginine-methylated proteins. The detected banding pattern in the immunoblot observed shares similarities to the silver-stained gels of the immunoprecipitation eluates in panel A. As immunoprecipitations can pull down nonarginine-methylated interaction partners of arginine-methylated proteins, the banding pattern we observe is not completely identical. However, this result suggests that the proteins that were immunoprecipitated include arginine-methylated proteins.

WXXXR motifs from Pang et al.,<sup>42</sup> and the RXR motif from Smith et al.<sup>43</sup> The RGG motif is the canonical triplet motif known to be arginine-methylated while the WXXXR and GXXX motifs have been recently described as methylated in yeast.<sup>42</sup> The RXG, RGX, and RXR motifs shown to be methylated by PRMT1,<sup>41,43</sup> the human homologue of Hmt1, were also included in the search. Functional annotation enrichment analyses were done using the Database for Annotation, Visualization and Integrated Discovery (DAVID) version 6.7.<sup>44</sup> The “GOTERM\_XX\_FAT” categories were used, where “XX” was either BP (biological process), CC (cellular component), or MF (molecular function). Default settings were used at all times, redundant terms were excluded, and the modified Fisher’s Exact statistic are shown (Table S4 of the Supporting Information).

## RESULTS

### Survey of the *S. cerevisiae* Proteome for Arginine Methylation

Two affinity-purified antibodies, raised against either monomethylarginine (MMA) or asymmetric dimethylarginine (aDMA), were used to detect the presence of arginine methylation in the *S. cerevisiae* proteome. From the immunoblots of the wild-type yeast cell extracts, the antibodies detected a total of 55 proteins over a wide range of molecular weights (Figure 1). Among this, 12 bands (at 80, 68, 63, 57, 55, 53, 47, 39, 37, 24, 20, and 16 kDa) for the anti-MMA blots and 15 bands (at 98, 80, 63, 57, 55, 53, 47, 44, 40, 39, 37, 29, 26, 24, and 20 kDa) for the anti-aDMA blots were seen as major proteins (arrowed, Figure 1). The remainder were considered as minor bands. Of the major bands detected, 10 of these (80, 63, 57, 55, 53, 47, 39, 37, 24, and 20 kDa) were detected by both antibodies.

### Arginine Methyltransferase Gene Deletion Mutants Show Loss of Methylation

To investigate the arginine methyltransferases responsible for methylation in the *S. cerevisiae* proteome, gene deletion mutants of known arginine methyltransferases (Hmt1, Rmt2, and Hsl7) were analyzed. Single gene deletions from the *S. cerevisiae* Genome Deletion Project<sup>25,26</sup> were PCR-verified before use or constructed in the haploid *S. cerevisiae* BY4741 by PCR-based targeted gene deletion<sup>27</sup> (Figures S1 and S2 of the Supporting Information). To investigate possible redundancy between the arginine methyltransferases and understand if arginine methylation is essential in yeast, combinatorial double and triple gene deletion mutants were also generated (Figure S3 of the Supporting Information).

After the gene deletion mutants were constructed, immunoblots were performed against whole cell lysates. Through these immunoblots, we aimed to elucidate the enzyme–substrate links between the methyltransferases and the protein bands detected. For this purpose, both the anti-MMA and anti-aDMA antibodies were used (Figure 2). We observed that deletion of the *HMT1* gene had the most significant effect on the methylation of *S. cerevisiae* proteins, while the deletion of the *RMT2* or *HSL7* genes appeared to have no observable effects. Bands that were clearly observed to be missing in the *hmt1* knockout, using the anti-MMA antibodies, included proteins of 57, 55, 53, 39, and 24 kDa (arrowed, Figure 2A). Most interestingly, extensive arginine methylation of proteins was still observed despite the deletion of 3 known arginine methyltransferases in the triple knockout mutant strain. When lysates were analyzed with the anti-aDMA antibodies, a large number of bands were observed (Figure 2B). Differences were observed in the *hmt1* knockout at the major bands of 53, 39, and 24 kDa (arrowed, Figure 2B).

Having observed that protein arginine methylation was apparently widespread, it was important to check the specificity of the antibodies used. To this end, we subjected the antibodies and immunoblots to competitive inhibition (Figure 3). Here, during primary antibody incubation, either free unmodified or modified arginines were added as competitive inhibitors. We observed that the anti-MMA antibody was almost completely inhibited in the presence of free MMA, while much less inhibition was observed in the presence of free aDMA or sDMA, with sDMA showing the least inhibitory effect (Figure 3A). Importantly, free unmodified arginine was not inhibitory to the anti-MMA antibody. These results suggest that the anti-MMA antibody is specific to methylarginines and has the highest affinity to monomethylarginine. In contrast to the anti-MMA



Table 2. List of Proteins Selected for Validation

gene name	name description	molecular function <sup>a</sup>	potential methyl-R sites <sup>b</sup>	mass (with tags) kDa <sup>c</sup>
<b>wild-type</b>				
<i>DED1</i> <sup>d</sup>	ATP-dependent RNA helicase DED1	RNA/ATP binding, helicase	22	65 (83)
<i>IMD4</i>	inosine-5'-monophosphate dehydrogenase 4	oxidoreductase, protein binding	7	56 (73)
<i>LHP1</i>	La protein homologue	RNA/protein binding	3	32 (49)
<i>NOPI</i> <sup>e</sup>	rRNA 2'-O-methyltransferase fibrillarin	RNA binding, methyltransferase	22	34 (52)
<i>NOP6</i>	nucleolar protein 6	RNA binding	4	25 (42)
<i>PRT1</i>	eukaryotic translation initiation factor 3 subunit B	RNA/protein binding	7	88 (105)
<b>arginine methyltransferase triple knockout mutant</b>				
<i>ARC1</i>	GU4 nucleic-binding protein 1	RNA/lipid binding, enzyme activator	3	42 (59)
<i>CBF5</i>	H/ACA ribonucleoprotein complex subunit 4	RNA/protein binding, isomerase	7	54 (72)
<i>CDC11</i>	cell division control protein 11	GTP/lipid/protein binding, structural molecule	7	47 (65)
<i>GUS1</i>	glutamate-tRNA ligase, cytoplasmic	tRNA-ligase	14	80 (98)
<i>PAB1</i>	poly(A)-binding protein	RNA binding	3	64 (81)
<i>POB3</i>	FACT complex subunit POB3	Histone binding	11	62 (80)
<i>RF1</i>	replication factor A protein 1	DNA/protein binding	10	70 (87)
<i>UGP1</i>	UTP-glucose-1-phosphate uridylyltransferase	nucleotidyltransferase, protein binding	8	55 (73)

<sup>a</sup>Summarized molecular function GO terms were sourced from SGD<sup>38</sup> and from the Uniprot Consortium.<sup>39</sup> <sup>b</sup>The RXG and RGX motifs are from Wooderchak et al.;<sup>41</sup> GXXR and WXXR motifs are from Pang et al.;<sup>42</sup> RXX motif is from Smith et al.<sup>43</sup> <sup>c</sup>Calculated molecular weight in kDa. Associated C-terminal tags were ~17 kDa. <sup>d</sup>Ded1 protein sequence was found to have 4 RGG motifs, a motif methylated by Hmt1. It was thus selected to be under "wild-type". <sup>e</sup>Nop1 served as a positive control.

antibody, the anti-aDMA antibody showed no significant inhibition in the presence of both unmodified and modified arginines (Figure 3B). The competitive inhibition results suggest that the anti-aDMA antibody is not specific to methylarginines.

During the drafting of this manuscript, Sfm1 was shown to be an arginine methyltransferase.<sup>11</sup> As a result, the *sfm1* deletion mutant was obtained, PCR-verified, and its methylation profile compared to the wild-type strain in an immunoblot blot using the anti-MMA antibody (Figure S6 of the Supporting Information). Because no differences were observed in the immunoblot, we did not pursue the use of this mutant further in this work.

### Immunoprecipitation to Enrich for Methylarginine-Containing Proteins

The observation of a large number of bands in the immunoblots is interesting, as only 20 methylarginine-containing proteins in *S. cerevisiae* have been described to date.<sup>18</sup> Immunoprecipitations were performed with the anti-MMA antibody for both the wild-type and the arginine methyltransferase triple knockout mutant; these were compared to a control anti-HA antibody pulldown (Figure 4A). Immunoprecipitated proteins were expected to be a mix of methylarginine-containing proteins and their nonmethylated but functionally related interaction partners. Immunoblots using the same anti-MMA antibody against the immunoprecipitates demonstrated modest enrichment of methylarginine-containing proteins (Figure 4B). Analysis of the immunoblots and the silver-stained SDS-PAGE gel (Figure 4) showed that the antimethylation immunoprecipitates shared a large number of protein bands, such as in the region between 40 kDa to 70 kDa and between 16 kDa to 25 kDa. The wild-type immunoprecipitate contained many proteins, with fairly even distributions of quantities. By contrast, the precipitates from the arginine methyltransferase triple knockout mutant had fewer bands, such as in the 35 kDa region. While there were several

bands present in the negative control, most of these bands do not correspond to those observed in the wild type or mutant lanes, except a band at 41 kDa.

When the immunoprecipitated protein bands were compared to an immunoblot of cell extracts probed with the same anti-MMA antibody, we observed similar major bands in the 63, 57, 53, 24, 20, and 16 kDa regions (Figures 1 and 4), while additional bands were seen at 160, 49, 43, 41, and 35 kDa (Figure 4), only in the immunoprecipitates. Similarities between the immunoblots and the immunoprecipitates were expected as the same antibody was used for both experiments.

### Identification of Proteins from Immunoprecipitates

Post SDS-PAGE, protein bands were excised and subjected to liquid chromatography-tandem mass spectrometry (LC-MS/MS) and database searching using Mascot (Matrix Science). Bands from the control anti-HA antibody immunoprecipitate were also analyzed (Table S3 of the Supporting Information). After filtering out proteins from the control, a total of 55 proteins were identified from the wild-type and 50 for the arginine methyltransferase triple knockout mutant (Table 1). Among the proteins identified from the immunoprecipitates of the wild-type strain, four known Hmt1 arginine-methylated substrates, Nop1, Nsr1, Sbp1, and Yra1 (Table 1), were identified. The well-documented Hmt1 substrate Npl3 was also identified in the wild-type sample; however, this is not included in Table 1, as it was also found in the negative control (Table S3 of the Supporting Information). The immunoprecipitates from the arginine methyltransferase triple knockout mutant had three known methylarginine substrates, namely Nop1, Nsr1, and Rps3 (Table 1). The observation of Rps3 from the triple knockout mutant was of particular note, as it was recently reported as a substrate of the newly identified arginine methyltransferase Sfm1.<sup>11</sup> The presence of the first two proteins (Nop1 and Nsr1) was



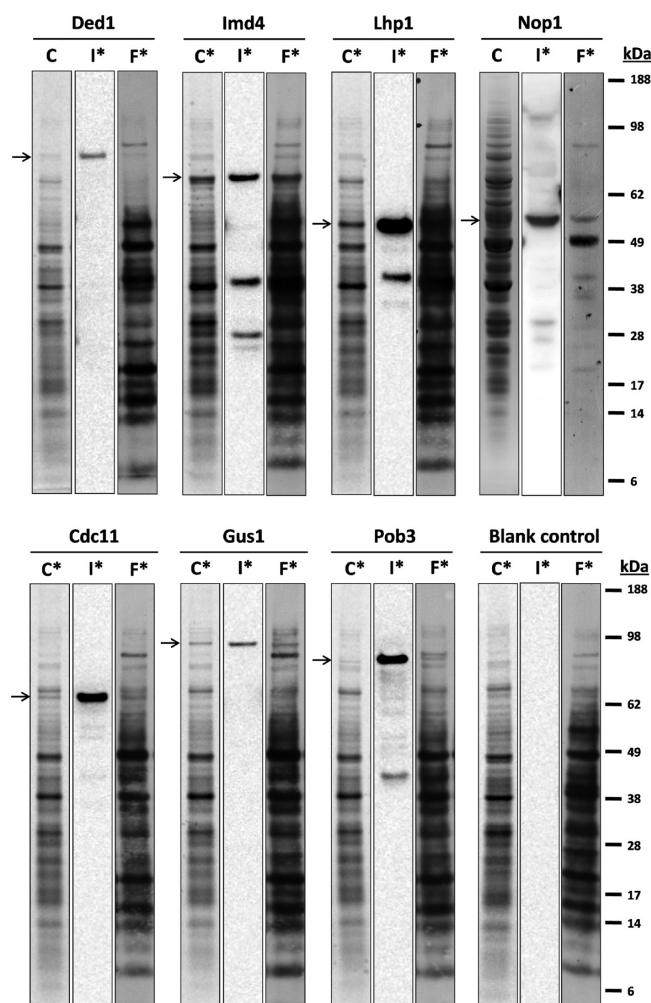


**Figure 5.** Seven validation candidates show in vivo methylation. Each validation candidate has three gel lanes: a Coomassie-stained gel (C), a corresponding immunoblot (I), and a fluorograph from the radiolabeling (F). Immunoblots were performed to aid the detection of the expressed protein, and the anti-His antibodies were used. Arrows on the left denote the position where the expressed protein of interest has been observed and the presence of an asterisk (\*) above the lanes denote if the protein has been observed in that lane. A total of seven tested candidates, including the positive control (Nop1), were observed to be methylated in vivo. Ded1, Imd4, Lhp1, and Nop1 shown above were expressed in wild type *S. cerevisiae*, while Cdc11, Gus1, and Pob3 were expressed in the arginine methyltransferase triple knockout mutant. The negative control without an overexpressed protein is for referencing the background methylation levels. The Nop1 fluorograph was from a repeated experiment with reduced radiolabels (Figure S8C of the Supporting Information and Methods). Full-sized images of the stained gels, immunoblots, and fluorographs are available as Figures S7–S10 of the Supporting Information.

unexpected in the triple knockout as they are known substrates of Hmt1. However, it is possible that in the absence of Hmt1 they were methylated by another methyltransferase; the high degree of methylation that remains in the triple knockout and the fact that it can be out-competed by free MMA in immunoblots is consistent with this hypothesis (Figures 2A and 3A). The overall identification of five known substrates in the immunoprecipitates, of the 20 previously described in *S. cerevisiae*, illustrates the utility of our approach, although it must be kept in mind that interaction partners of methylarginine-containing proteins are

also likely to be present in the immunoprecipitates and that these may not necessarily contain methylarginine.

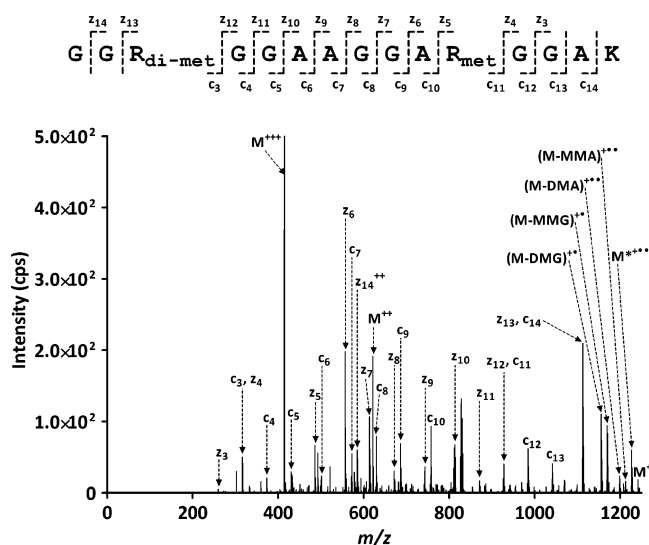
Among the 55 proteins found in the wild-type sample, 54 were of known localization (Table 1). All 54 proteins could be found in two major locations, in either the cytoplasm or the nucleus. When classified into either of these two locations, 64.8% were found in the cytoplasm, 16.6% in the nucleus, while 18.5% were found in both locations. Similarly, among the 50 proteins identified in the triple knockout mutant, 49 were of known localization and could be classified into either the nucleus or cytoplasm (Table 1). In this set, 69.3% were found to localize to the cytoplasm, 20.4% to the nucleus, while 10.2% to both locations. A proportion of the identified proteins were also observed to localize to other subcellular locations, such as the mitochondria, cell membrane, and, to a lesser extent, the vacuole. This finding agrees with the literature that *S. cerevisiae* arginine-methylated proteins have diverse cellular localization patterns but are mainly found in the cytoplasm and nucleus.<sup>18</sup> Interestingly, we also note that there is almost twice the proportion of identified proteins that could localize to both the cytoplasm as well as the nucleus in the wild-type sample compared to the mutant sample. This is in accordance with the observation that Hmt1 (present in the wild-type sample) is currently the sole methyltransferase responsible for the methylation of shuttling hnRNPs.<sup>23,45–47</sup>

Protein sequences of the immunoprecipitated proteins were analyzed to identify putative methylation sites based on previously described motifs (see Methods for details). From this analysis, we found 84 of the 90 unique proteins had at least 1 putative methylation site with an average of 5.6 sites per protein and a median of 5 sites (Table 1). As an example, Npl3 has been previously reported to have 19 methylarginine sites.<sup>34,48</sup> This is close to the 24 potential sites predicted using the method employed here. Apart from known arginine-methylated substrates, many other proteins not previously reported to be arginine-methylated were found to have a large number of putative sites in this study. These included Ded1, Dur1,2, Gus1, and Rps5, each with 22, 21, 14, and 14 putative sites, respectively. Proteins with five or more potential sites are highlighted in Table 1.

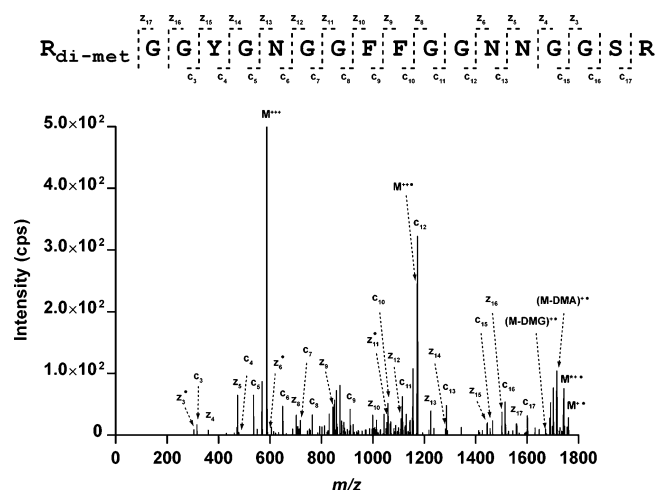
Functional enrichment, using gene ontology (GO), was carried out for the identified proteins (Table S4 of the Supporting Information). As mentioned above, we do not expect all identified proteins to contain methylarginines, as immunoprecipitations can also pull down nonarginine-methylated interaction partners of arginine-methylated proteins. Nevertheless, function enrichment analysis will be informative as the interaction partners of methylarginine-containing proteins will be functionally related.<sup>49</sup> Significant GO biological processes, when compared to those shown by the negative control, included known methylarginine-associated processes such as “ribosome biogenesis” (wild-type  $p = 7.3 \times 10^{-10}$ , mutant  $p = 1.3 \times 10^{-7}$ , and control  $p =$  not significant), “nucleocytoplasmic transport” (wild-type  $p = 9.5 \times 10^{-4}$ , mutant  $p = 3.7 \times 10^{-2}$ , and control  $p =$  not significant), and “translation” (wild-type  $p = 2.5 \times 10^{-15}$ , mutant  $p = 6.8 \times 10^{-7}$ , and control  $p = 6.8 \times 10^{-12}$ ). The top-ranked GO molecular functions and cellular components also mapped to a series of RNA-binding and processing-associated terms (Table S4 of the Supporting Information). Note that although “translation” was also seen in the control, in the wild-type sample, the  $p$ -value is more than 3 orders of magnitude less than the control.

Table 3. List of Methylarginine-Containing Peptides found using MS/MS

peptide sequence <sup>a</sup>	residues	observed monoisotopic <i>m/z</i> (charge)	mascot ion score	expect ( <i>E</i> -value)	modification
<b>Nop1</b>					
GG <u>R</u> GGAAGGARGGAK	71–85	414.5654 (+3)	73	$1.2 \times 10^{-5}$	dimethyl (R3), methyl (R11)
GGAAGGAR <u>G</u> GAK	74–85	472.2569 (+2)	56	$3.7 \times 10^{-4}$	methyl (R8)
GGAAGGAR <u>G</u> GAK	74–85	479.2662 (+2)	40	$1.3 \times 10^{-2}$	dimethyl (R8)
GGS <u>R</u> GGRGGAAGGAR	67–81	424.5605 (+3)	50	$2.4 \times 10^{-3}$	methyl (R4), methyl (R7)
GGS <u>R</u> GGRGGAAGGAR	67–81	433.9045 (+3)	34	$2.1 \times 10^{-2}$	dimethyl (R4), dimethyl (R7)
GG <u>R</u> GGAAGGAR	71–81	450.7418 (+2)	41	$7.4 \times 10^{-3}$	methyl (R3)
GG <u>R</u> GGAAGGAR	71–81	457.7492 (+2)	45	$6.0 \times 10^{-3}$	dimethyl (R3)
GG <u>A</u> RGGS <u>R</u> GGFGGR	27–40, 45–58	435.5691 (+3)	43	$6.2 \times 10^{-3}$	dimethyl (R4), dimethyl (R8)
GG <u>S</u> RGFGGRGGS	13–26, 31–44, 49–62	653.8408 (+2)	27	$4.3 \times 10^{-2}$	dimethyl (R4), methyl (R10)
GG <u>S</u> RGFGGR	13–22, 31–40, 49–58	461.2361 (+2)	36	$2.9 \times 10^{-2}$	methyl (R4)
<b>Ded1</b>					
<u>R</u> GGYGNGGFFGGNNGGS	62–79	586.9396 (+3)	62	$2.6 \times 10^{-5}$	dimethyl (R1)
<b>Lhp1</b>					
SSEILEVSADGENVK <u>R</u>	89–104	873.9489 (+2)	44	$8.0 \times 10^{-4}$	methyl (R16)
<b>Pab1</b>					
AIEQLNYTPIK <u>R</u>	95–107	758.9280 (+2)	31	$1.6 \times 10^{-2}$	methyl (R13)
<b>Ugp1</b>					
DGHEINVQLLETACGA <u>A</u> I <u>R</u>	351–369	1041.0280 (+2)	34	$1.9 \times 10^{-3}$	methyl (R19)

<sup>a</sup>Modification sites are underlined.

**Figure 6.** ETD-MS/MS of an in vivo methylated Nop1 peptide at 414.5654 *m/z* identifies two methylarginine sites. Nop1, overexpressed and in vivo methylated in wild-type *S. cerevisiae*, was subjected to ETD-MS/MS. Shown in the figure is the annotated ETD-MS/MS spectrum obtained for the triply charged tryptic Nop1 peptide GGR(dimethyl)-GGAAGGAR(monomethyl)GGAK observed at 414.5654 *m/z*. Included above is the summarized fragment-ion coverage where observed *c* and *z* ions and their derivatives are shown. In this peptide, two methylarginine sites were identified (residues 3 and 11). A near complete *c*- and *z*-ion series was observed (24 out of 28 possible *c* and *z* ions). As a result, fragment-ions covering the sequence before and after the methylarginine sites were identified and a high Mascot ion score of 73 (*E*-value =  $1.2 \times 10^{-5}$ ) was reported. Importantly, diagnostic neutral losses specific for methylarginines were also observed. The observation of the near-complete *c*- and *z*-ion series and the diagnostic neutral losses confirmed the presence of a dimethylarginine at residue 3 and a monomethylarginine at residue 11. Precursor ions, charge-reduced ions (denoted by ●), methylation-specific neutral losses, *c* and *z* ions are labeled in the spectrum.



**Figure 7.** ETD-MS/MS of an in vivo methylated Ded1 peptide at 586.9396 *m/z* identifies a dimethylarginine site. Ded1, overexpressed and in vivo methylated in wild-type *S. cerevisiae*, was subjected to ETD-MS/MS. Shown in the figure is the annotated ETD-MS/MS spectrum obtained for the triply charged tryptic Ded1 peptide R(dimethyl)GGYGNGGFFGGNNGGS observed at 586.9396 *m/z*. Included above is the summarized fragment-ion coverage where observed *c* and *z* ions and their derivatives are shown. In this peptide, one methylarginine site was identified (residue 1). A near complete *c* and *z* ion series was observed (28 out of 34 possible *c* and *z* ions). As a result, 14 out of 17 possible *c* ions carrying the methylarginine site were identified and a high Mascot ion score of 62 (*E*-value =  $2.6 \times 10^{-5}$ ) was reported. Importantly, diagnostic neutral losses specific for methylarginines were also observed. The observation of the near-complete *c*- and *z*-ion series and the diagnostic neutral losses confirmed the presence of a dimethylarginine at residue 1. Precursor ions, charge-reduced ions (denoted by ●), methylation-specific neutral losses, *c* and *z* ions are labeled in the spectrum.

Importantly, we observed that some of our identified proteins were associated with biological processes and molecular

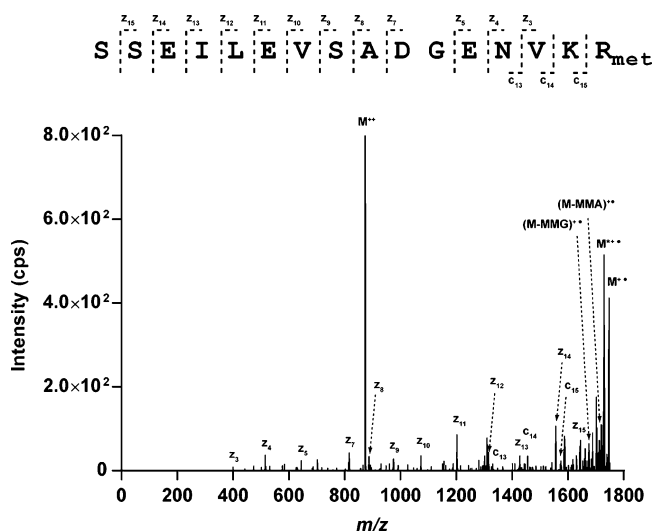


**Figure 8.** ETD-MS/MS of an in vivo methylated Lhp1 peptide at 873.9489  $m/z$  identifies a monomethylarginine site. Lhp1, overexpressed and in vivo methylated in wild-type *S. cerevisiae*, was subjected to ETD-MS/MS. Shown in the figure is the annotated ETD-MS/MS spectrum obtained for the doubly charged tryptic Lhp1 peptide SSEILEVSADGENVKR(monomethyl) observed at 873.9489  $m/z$ . Included above is the summarized fragment-ion coverage where observed  $c$  and  $z$  ions and their derivatives are shown. In this peptide, one methylarginine site was identified (residue 16). A near complete  $z$  ion series carrying the methylarginine site was observed (12 out of 15 possible  $z$  ions). As a result, a good Mascot ion score of 44 ( $E$ -value =  $8.0 \times 10^{-4}$ ) was reported. Importantly, diagnostic neutral losses specific for methylarginines were also observed. The observation of the near-complete  $z$ -ion series and the diagnostic neutral losses confirmed the presence of a monomethylarginine at residue 16. Precursor ions, charge-reduced ions (denoted by  $\bullet$ ), methylation-specific neutral losses, and  $c$  and  $z$  ions are labeled in the spectrum.

functions not strongly associated with arginine methylation. These include “glycolysis” (Table S4 of the Supporting Information, biological process, wild-type  $p = 7.2 \times 10^{-4}$ , mutant  $p = 1.4 \times 10^{-6}$ , and control  $p = 1.0 \times 10^{-3}$ ), “protein refolding” (Table S4 of the Supporting Information, biological process, wild-type  $p = 7.2 \times 10^{-5}$ , mutant and control  $p =$  not significant), and “structural constituent of cytoskeleton” (Table S4 of the Supporting Information, molecular function, mutant  $p = 3.1 \times 10^{-2}$ , wild type and control  $p =$  not significant).

#### Validation of Arginine Methylation

A total of 14 proteins identified from our immunoprecipitation experiments were selected for validation (Table 2 and Methods of the Supporting Information). Many proteins were selected as representative of novel functional classes; these included a helicase (Ded1), tRNA-ligase (Gus1), DNA binding proteins (Rfa1 and Pob3), an oxidoreductase (Imd4), and a cytoskeletal protein (Cdc11). These proteins also had a large number of potential methylation sites (7 or more; Table 1). Other proteins (e.g., Nop6, Pab1, and Cbf5) were of interest, as they were RNA-binding and thus likely to be methylated. Nop1, a known Hmt1 substrate, was selected as the positive control (for the complete listing see Table 2 and for detailed selection criteria see Methods of the Supporting Information). Validation was achieved in two ways, primarily through the use of overexpressed proteins. First, in vivo methylation of target proteins was undertaken using tritium-labeled S-adenosyl-L-methionine ( $[^3H]$ -SAM) and detection by fluorography. The in vivo methylation of target

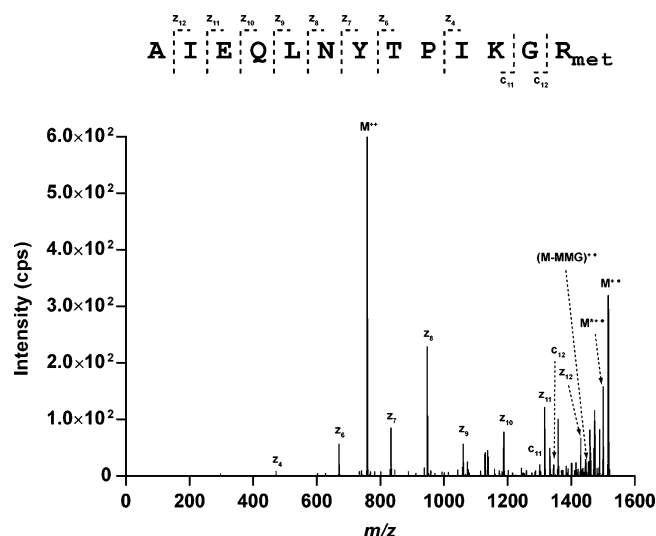


**Figure 9.** ETD-MS/MS of an in vivo methylated Pab1 peptide at 758.9280  $m/z$  identifies a monomethylarginine site. Pab1, overexpressed and in vivo methylated in the arginine methyltransferase triple knockout mutant strain of *S. cerevisiae*, was subjected to ETD-MS/MS. Shown in the figure is the annotated ETD-MS/MS spectrum obtained for the doubly charged tryptic Pab1 peptide SAIEQLNYTPIKGR(monomethyl) observed at 758.9280  $m/z$ . Included above is the summarized fragment-ion coverage where observed  $c$  and  $z$  ions and their derivatives are shown. In this peptide, one methylarginine site was identified (residue 13). A near complete  $z$  ion series carrying the methylarginine site was observed (8 out of 11 possible  $z$  ions). As a result, a good Mascot ion score of 31 ( $E$ -value =  $1.6 \times 10^{-2}$ ) was reported. Importantly, diagnostic neutral losses specific for methylarginines were also observed. The observation of the near-complete  $z$ -ion series and the diagnostic neutral losses confirmed the presence of a monomethylarginine at residue 13. Precursor ions, charge-reduced ions (denoted by  $\bullet$ ), methylation-specific neutral losses,  $c$  and  $z$  ions are labeled in the spectrum.

proteins is possible due to the active uptake of SAM by *S. cerevisiae*.<sup>50</sup> Despite the possibility of radiolabeling other targets (e.g., lysine and histidine), arginine methylation has been shown to be the dominant form; ~90% of all methylation events in rat cells were of this type.<sup>51</sup> Second, methylarginine site identification was done via mass spectrometry.

From the overexpression and in vivo methylation validation experiments, a total of seven proteins (Cdc11, Ded1, Gus1, Imd4, Lhp1, Nop1, and Pob3), including the positive control, were found to be methylated (Figure 5 and Figures S7–S10 of the Supporting Information). The identities of these proteins were confirmed by CID MS/MS (data not shown). Sites of methylation were then sought by electron-transfer dissociation (ETD), and in some cases CID MS/MS. A total of 14 different methylarginine-containing peptide ions were found for five proteins (Nop1, Ded1, Lhp1, Pab1, and Ugp1; Table 3). Eleven methylarginine sites were found on Nop1 and one site for each of the remaining four proteins; all sites found are novel. In each peptide MS/MS spectrum, substantial peptide coverage by fragment ions was seen, allowing the methylarginine site to be localized. Importantly, for most MS/MS spectra (12 out of 14), diagnostic methylarginine-specific neutral losses were also observed (Figures 6–10, and Figures S11–S19 of the Supporting Information).<sup>37</sup> The sites on Nop1 and Ded1 were present in the canonical Gly–Arg rich motif, whereas those from Lhp1, Pab1, and Ugp1 were not present in this type of motif or any other motif included in our predictions. The location of the large



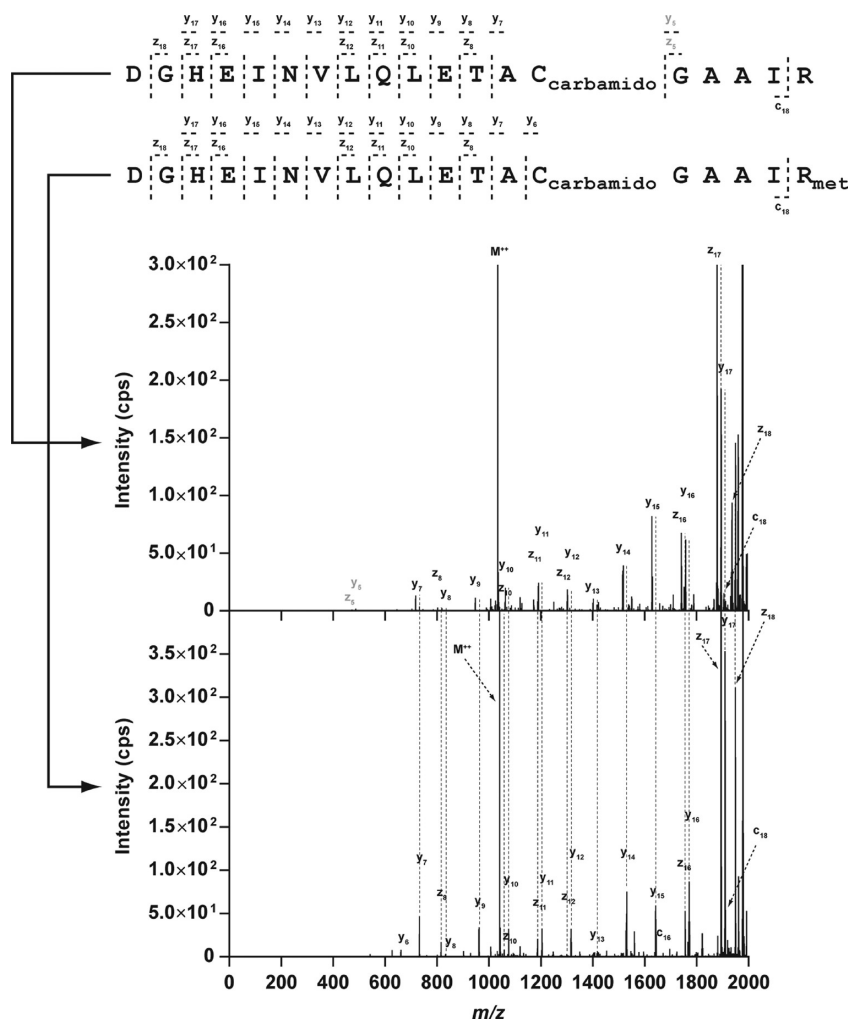


**Figure 10.** MS/MS of an in vivo methylated Ugp1 peptide at 1041.0280  $m/z$  identifies a monomethylarginine site. Ugp1, overexpressed and in vivo-methylated in the arginine methyltransferase triple knockout mutant strain of *S. cerevisiae*, was subjected to ETD-MS/MS with supplemental CID activation. Shown in the figure is the annotated MS/MS spectrum obtained for the doubly charged tryptic Ugp1 peptide DGHEINVLQLETAC-(carbamidomethyl)GAAIR(monomethyl) observed at 1041.0280  $m/z$ . For comparison purposes, the corresponding doubly charged unmethylated peptide observed at 1034.0180  $m/z$  has been included. Shown above the spectra are the summarized fragment-ion coverage where observed  $c$ ,  $z$ , and  $y$  ions and their derivatives are shown. In this peptide, one methylarginine site was identified (residue 19). A total of 19  $z$  and  $y$  ions, out of the possible 36, carrying the methylarginine site was observed. As a result, a significant Mascot ion score of 34 ( $E$  value =  $1.9 \times 10^{-3}$ ) was reported. Diagnostic neutral losses specific for methylarginines could not be observed as they had  $m/z$  (s) beyond the mass spectrometer's employed mass range. Instead, by comparing the methylated and unmethylated peptide spectra, mass shifts of 14 Da, corresponding to the addition of a methyl group, can be observed for 18 of the  $z$  and  $y$  ions. The observations of a series of methylarginine-carrying fragment ions and the mass shifts between the methylated and unmethylated spectra supports the presence of a monomethylarginine at residue 19. Precursor ions, charge-reduced ions (denoted by ●), methylation-specific neutral losses,  $c$ ,  $z$ , and  $y$  ions are labeled in the spectrum. The unmethylated peptide had a Mascot score of 32 ( $E$ -value =  $5.0 \times 10^{-3}$ ).

number of sites identified for Nop1 are summarized in Figure 11. Of the 5 proteins not validated to contain methylarginines, three were poorly or not expressed (Cbf5, Prt1, Rfa1) and two candidates (Arc1 and Nop6) were expressed but not confirmed to contain methylarginines (Figures S9 and S10 of the Supporting Information).

Among the nine validated candidates, we observed proteins involved in new biological processes not previously associated with arginine methylation. These included the cytoskeleton/cell cycle-associated protein Cdc11, the GMP/metabolite biosynthesis-associated protein Imd4, and the nucleotidyltransferase Ugp1. In addition, proteins from functional classes previously not strongly associated with arginine methylation, such as Gus1 (tRNA ligase) and Ded1 (helicase), were also validated. The proteins described above are the first of their type found to be methylated in *S. cerevisiae*. It is noteworthy that there have been

three reports of arginine-methylated helicases in other species, bringing the overall total to four.<sup>52–54</sup>

## DISCUSSION

In the present study, we surveyed the extent of arginine methylation in the *S. cerevisiae* proteome. The prior use of methylation-specific antibodies in the study of arginine-methylated proteins has been limited to the detection of single proteins or peptides.<sup>20,22–24</sup> Here, we tested and showed through the use of competitive assays that the anti-MMA antibody is predominantly specific for MMA, while an anti-dMA antibody, though able to detect methylarginines, also has affinity toward other unknown epitopes. From the use of anti-MMA immunoblotting, a large number of arginine-methylated proteins were seen in the yeast proteome. By IP and LC-MS/MS, a total of 55 proteins from the wild-type samples and

## Nop1

1 MSFRPGSRGG SRGGS<sup>\*</sup>RGGFG GRGGS<sup>o</sup>RGGAR GGS<sup>\*</sup>RGGFGGR GGS<sup>o</sup>RGGARGG SRGGFG<sup>o</sup>RGG SRGGARGGS<sup>\*</sup>

71 GGRGGAAGGA<sup>\*</sup> RGGAKVVIEP<sup>\*</sup> HRHAGVYIAR GKEDLLVTKN MAPGESVYGE KRISVEEPSK EDGVPPTKVE

141 YRVWNPFRSK LAAGIMGGGLD ELFIAPGKKV LYLGAASGTS VSHVSDVVGP EGVVYAVEFS HRPGRELISM

211 AKKRPNIIFI IEDARHPQKY RMLIGMVDCV FADVAQPDQA RIIALNSHMF LKDQGGVVIS IKANCIDSTV

281 DAETVFAREV QKLREERIKP LEQLTLEPYE RDHCIVVGRY MRSGLKK

\* = mono- and dimethylarginine site

o = monomethylarginine site only

• = dimethylarginine site only

**Figure 11.** Summary of methylarginine sites identified in Nop1 using MS/MS. A total of 11 sites were identified in Nop1. Methylated Nop1 samples were generated via overexpression in wild-type *S. cerevisiae* and methylated in vivo. Amino acids observed in tryptic peptides are shown in black. Apart from their unmethylated states, sites observed to be exclusively monomethylated are denoted by a “o” symbol above the residue, while exclusively dimethylated sites are denoted by the “•” symbol. Sites observed to be mono- and dimethylated have the “\*” symbol. All sites described here are novel.

50 proteins from the arginine methyltransferase triple knockout mutant were identified, resulting in a total of 90 unique proteins. The identification of 5 known arginine-methylated proteins among the 90 proteins illustrated the utility of our experimental approach, although it must be noted that some of the 90 proteins will be interaction partners of arginine-methylated proteins and thus not necessarily methylated. The remaining 85 proteins reported here, the majority of which require further investigation to confirm the presence of methylation, have the potential to contribute to a significant advance over the 20 methylarginine proteins currently described.<sup>18</sup>

Nine proteins, including a positive control Nop1, were validated and shown to be methylated in vivo. Three of the verified proteins, Ded1, Cdc11, and Gus1, were previously predicted but not shown to be methylated.<sup>33,42</sup> In addition, a paralog of validated protein Imd4 and Imd3, was also predicted to be methylated by Pang et al.,<sup>42</sup> and mammalian homologues of Pab1 have been previously described to be methylated.<sup>55</sup> Through MS/MS, we report the identification of a total of 15 novel methylarginine sites on Nop1, Ded1, Lhp1, Pab1 and Ugp1. Eleven of these sites were on Nop1; sites for Nop1 have not previously been mapped, despite it being a known Hmt1 substrate.<sup>33</sup> For Ded1, Lhp1, Pab1 and Ugp1, this is the first report of methylation and sites for these proteins. While the sites on Nop1 and Ded1 were present in canonical RGG motifs, those from Lhp1, Pab1 and Ugp1 were not present in this glycine-arginine rich motif nor any other motif included in our predictions. It is possible that these methylarginine sites are within novel motifs, however, we are not able to perform a consensus site search with the current, small number of identified non-RGG methylarginine sites.

Functional enrichment analysis of all identified proteins, including those that may be functionally related interaction partners of those with arginine methylation, showed that the major biological processes of these proteins, such as ribosome biogenesis, RNA processing, and nucleocytoplasmic transport, were consistent with those already known for *S. cerevisiae* (reviewed in 18). Interestingly, functional enrichment analysis also identified biological processes and molecular functions involving GMP biosynthesis, protein folding, glycolysis, and the cytoskeleton. These biological processes have not previously been strongly associated with arginine methylation in *S. cerevisiae*. However, recent bioinformatic work done in our laboratory did

identify several putative proteins (e.g., heat shock chaperones, tubulins, and enzymes involved in GMP biosynthesis) that are from these biological processes.<sup>42</sup> Similarly, in an immunoprecipitation followed by LC–MS/MS experiment on HeLa cell extracts, novel DNA repair, and cytoskeleton proteins were identified to be putatively arginine-methylated.<sup>19</sup> One of the identified DNA repair proteins from that study, MRE11, has since been verified to be methylated, and the effect of arginine methylation on its function has been elucidated (reviewed in 15). When this evidence is considered, it suggests that the newly identified biological process could represent unexplored classes of arginine-methylated proteins. As part of the analysis performed, the protein sequences of the identified proteins were examined to identify putative methylation motifs. We found that many proteins not previously described to be arginine-methylated possessed a large number of potential sites. The predicted motifs in the sequences were instructive; 7 out of 9 validated proteins had 7 to 22 predicted sites. This suggests that further validation should focus on proteins that are predicted to have a substantial number of methylation motifs.

Through the use of immunoblots, we note that most gross changes in arginine methylation can be attributed to the deletion of Hmt1. This is congruent with the literature where Hmt1 has been proposed as responsible for the methylation of ~89% of all aDMA and ~66% of MMA as measured by the in vivo incorporation of radiolabeled methyl groups.<sup>8</sup> In contrast, the deletion of the *RMT2* or *HSL7* genes appeared to have no observable effects on the immunoblots. This lack of observable substrates for Rmt2 may be because it methylates the  $\delta$ -N-nitrogen of the guanidino group instead of the  $\omega$ -N-groups; this would not be observed in our experiments as the antibodies used were not specific for  $\delta$ -N-methylarginine. On the other hand, no in vivo substrate has been described to date for Hsl7 despite recent efforts.<sup>56,57</sup> This lack of reported in vivo substrates indicates that Hsl7 either methylates proteins that are of very low abundance or methylates its substrates under specific conditions that were not considered here.

Here, we successfully generated and analyzed all combinations of double and triple gene deletions of 3 arginine methyltransferases (Hmt1, Rmt2, and Hsl7) in *S. cerevisiae*. The viability of the arginine methyltransferase double knockouts is consistent with the recent synthetic genetic interactions study in *S. cerevisiae*.<sup>58</sup> Similarly, the *hmt1/hsl7/rmt2* triple knockout has

also been previously reported to be viable, however little description on the fitness of the mutant was provided.<sup>59,60</sup> Taken together, the viability of the deletion mutants suggests that arginine methylation is nonessential or methylation events catalyzed by Hmt1, Rmt2, and Hsl7 are nonessential. This nonessentiality of arginine methyltransferases is consistent with many methyltransferase enzymes characterized to date, with the exception of the human PRMT5<sup>61</sup> as well as PRMT1 and PRMT4/CARM1 under specific conditions (reviewed in 15). Intriguingly, we observed that the *hmt1/hsl7/rmt2* triple knockout mutant showed substantial arginine methylation and, from the validation experiments, five proteins (Cdc11, Gus1, Pab1, Pob3, and Ugp1) were verified to be methylated *in vivo* when expressed in the triple knockout mutant. Of these five proteins, methylarginine sites were unambiguously identified for Pab1 and Ugp1 that had been purified from the triple knockout mutant. Together with the observation of substantial ongoing arginine methylation in the triple knockout mutant, the fact that this can be outcompeted by MMA in immunoblot inhibition assays, and the fact that all sDMA, 11% of aDMA, and 34% of MMA methylation events are yet to be associated with any methyltransferase,<sup>8</sup> it strongly suggests the presence of additional unidentified methyltransferases in *S. cerevisiae*. During the drafting of this manuscript, Sfm1 was shown to be an arginine methyltransferase responsible for the monomethylation of Arg146 in Rps3.<sup>11</sup> The discovery of this new arginine methyltransferase underscores our finding. However, given that other ribosomal methyltransferases do not typically methylate nonribosomal proteins (e.g., the series of Rkm methyltransferases), this does not detract us from our original conclusion that there are more arginine methyltransferases to be described in *S. cerevisiae*.

## ■ ASSOCIATED CONTENT

### ■ Supporting Information

Tables of primers and plasmids used, proteins identified, functional enrichment analysis, list of peptides identified via immunoprecipitation. Figures of gene deletion mutants, immunoblots, fluorographic image, blotted gels, over-expressed proteins, CID MS/MS spectra. Excel and PDF of data. This material is available free of charge via the Internet at <http://pubs.acs.org>.

## ■ AUTHOR INFORMATION

### Corresponding Author

\*E-mail: [marc.wilkins@unsw.edu.au](mailto:marc.wilkins@unsw.edu.au). Tel: +61-2-9385-3633. Fax: +61-2-9385-1483.

### Notes

The authors declare no competing financial interest.

## ■ ACKNOWLEDGMENTS

We thank Mark Raftery, Ling Zhong, and Sydney Liu Lau for their maintenance of the mass spectrometers at the UNSW Bioanalytical Mass Spectrometry Facility. M.R.W., G.H.-S., and M.A.E. thank the Australian Research Council (ARC) for their financial support. J.K.K.L. acknowledges financial support from an Australian Postgraduate Award and the UNSW Research Excellence Award. Author contributions: Immunoblots, immunoprecipitations, validation experiments, data analyses and manuscript preparation were performed by J.K.K.L. The project was supervised by M.R.W. and M.A.E., G.H.-S. and M.R.W.

contributed to the manuscript preparation. All ETD-MS/MS mass spectrometry were performed by G.H.-S. CID-MS/MS mass was performed by G.H.-S. and M.A.E.

## ■ REFERENCES

- (1) Khoury, G. A.; Baliban, R. C.; Floudas, C. A. Proteome-wide post-translational modification statistics: Frequency analysis and curation of the swiss-prot database. *Sci. Rep.* **2011**, *1*, 1–5.
- (2) Webb, K. J.; Lipson, R. S.; Al-Hadid, Q.; Whitelegge, J. P.; Clarke, S. G. Identification of protein N-terminal methyltransferases in yeast and humans. *Biochemistry* **2010**, *49* (25), 5225–5235.
- (3) Wu, J.; Tolstykh, T.; Lee, J.; Boyd, K.; Stock, J. B.; Broach, J. R. Carboxyl methylation of the phosphoprotein phosphatase 2A catalytic subunit promotes its functional association with regulatory subunits *in vivo*. *EMBO J.* **2000**, *19* (21), 5672–5681.
- (4) Heurgué-Hamard, V.; Champ, S.; Mora, L.; Merkoulova-Rainon, T.; Kisselev, L. L.; Buckingham, R. H. The glutamine residue of the conserved GGQ motif in *Saccharomyces cerevisiae* release factor eRF1 is methylated by the product of the YDR140W gene. *J. Biol. Chem.* **2005**, *280* (4), 2439–2445.
- (5) Webb, K. J.; Zurita-Lopez, C. I.; Al-Hadid, Q.; Laganowsky, A.; Young, B. D.; Lipson, R. S.; Souda, P.; Faull, K. F.; Whitelegge, J. P.; Clarke, S. G. A novel 3-methylhistidine modification of yeast ribosomal protein Rpl3 is dependent upon the YIL110W methyltransferase. *J. Biol. Chem.* **2010**, *285* (48), 37598–37606.
- (6) Mattheakis, L. C.; Shen, W. H.; Collier, R. J. DPH5, a methyltransferase gene required for diphthamide biosynthesis in *Saccharomyces cerevisiae*. *Mol. Cell. Biol.* **1992**, *12* (9), 4026–4037.
- (7) Marr, R. S.; Blair, L. C.; Thorner, J. *Saccharomyces cerevisiae* STE14 gene is required for COOH-terminal methylation of a-factor mating pheromone. *J. Biol. Chem.* **1990**, *265* (33), 20057–60.
- (8) Gary, J. D.; Lin, W.-J.; Yang, M. C.; Herschman, H. R.; Clarke, S. The predominant protein-arginine methyltransferase from *Saccharomyces cerevisiae*. *J. Biol. Chem.* **1996**, *271* (21), 12585–12594.
- (9) Henry, M. F.; Silver, P. A. A novel methyltransferase (Hmt1p) modifies poly(A)+-RNA-binding proteins. *Mol. Cell. Biol.* **1996**, *16* (7), 3668–78.
- (10) DeLange, R. J.; Glazer, A. N.; Smith, E. L. Identification and location of  $\epsilon$ -N-trimethyllysine in yeast cytochromes c. *J. Biol. Chem.* **1970**, *245* (13), 3325–3327.
- (11) Young, B. D.; Weiss, D. I.; Zurita-Lopez, C. I.; Webb, K. J.; Clarke, S. G.; McBride, A. E. Identification of methylated proteins in the yeast small ribosomal subunit: A role for SPOUT methyltransferases in protein arginine methylation. *Biochemistry* **2012**, *51* (25), 5091–5104.
- (12) Sprung, R.; Chen, Y.; Zhang, K.; Cheng, D.; Zhang, T.; Peng, J.; Zhao, Y. Identification and validation of eukaryotic aspartate and glutamate methylation in proteins. *J. Proteome Res.* **2008**, *7* (3), 1001–1006.
- (13) Gary, J. D.; Clarke, S. RNA and protein interactions modulated by protein arginine methylation. *Prog. Nucleic Acid Res. Mol. Biol.* **1998**, *61*, 65–131.
- (14) Bachand, F. Protein arginine methyltransferases: From unicellular eukaryotes to humans. *Eukaryotic Cell* **2007**, *6* (6), 889–898.
- (15) Bedford, M. T.; Clarke, S. G. Protein arginine methylation in mammals: Who, what, and why. *Mol. Cell* **2009**, *33* (1), 1–13.
- (16) Blackwell, E.; Ceman, S. Arginine methylation of RNA-binding proteins regulates cell function and differentiation. *Mol. Reprod. Dev.* **2012**, *79* (3), 163–175.
- (17) Erce, M. A.; Pang, C. N. I.; Hart-Smith, G.; Wilkins, M. R. The methylproteome and the intracellular methylation network. *Proteomics* **2012**, *12* (4–5), 564–586.
- (18) Low, J. K. K.; Wilkins, M. R. Protein arginine methylation in *Saccharomyces cerevisiae*. *FEBS J.* **2012**, *279* (24), 4423–4443.
- (19) Boisvert, F. M.; Cote, J.; Boulanger, M. C.; Richard, S. A proteomic analysis of arginine-methylated protein complexes. *Mol. Cell. Proteomics* **2003**, *2* (12), 1319–30.
- (20) Boisvert, F.-M.; Côté, J.; Boulanger, M.-C.; Cl  roux, P.; Bachand, F.; Autexier, C.; Richard, S. Symmetrical dimethylarginine methylation



is required for the localization of SMN in Cajal bodies and pre-mRNA splicing. *J. Cell Biol.* **2002**, *159* (6), 957–969.

(21) Wu, C. C.; MacCoss, M. J.; Mardones, G.; Finnigan, C.; Mogelsvang, S.; Yates, J. R.; Howell, K. E. Organellar proteomics reveals golgi arginine dimethylation. *Mol. Biol. Cell* **2004**, *15* (6), 2907–2919.

(22) Lacoste, N.; Utley, R. T.; Hunter, J. M.; Poirier, G. G.; Côté, J. Disruptor of telomeric silencing-1 is a chromatin-specific histone H3 methyltransferase. *J. Biol. Chem.* **2002**, *277* (34), 30421–30424.

(23) McBride, A. E.; Weiss, V. H.; Kim, H. K.; Hogle, J. M.; Silver, P. A. Analysis of the yeast arginine methyltransferase Hmt1p/Rmt1p and its *in vivo* function. *J. Biol. Chem.* **2000**, *275* (5), 3128–3136.

(24) Siebel, C. W.; Guthrie, C. The essential yeast RNA binding protein Np13p is methylated. *Proc. Natl. Acad. Sci. U.S.A.* **1996**, *93* (24), 13641–6.

(25) Giaever, G.; Chu, A. M.; Ni, L.; Connelly, C.; Riles, L.; Veronneau, S.; Dow, S.; Lucau-Danila, A.; Anderson, K.; Andre, B.; Arkin, A. P.; Astromoff, A.; El Bakkoury, M.; Bangham, R.; Benito, R.; Brachat, S.; Campanaro, S.; Curtiss, M.; Davis, K.; Deutschbauer, A.; Entian, K.-D.; Flaherty, P.; Foury, F.; Garfinkel, D. J.; Gerstein, M.; Gotte, D.; Guldener, U.; Hegemann, J. H.; Hempel, S.; Herman, Z.; Jaramillo, D. F.; Kelly, D. E.; Kelly, S. L.; Kotter, P.; LaBonte, D.; Lamb, D. C.; Lan, N.; Liang, H.; Liao, H.; Liu, L.; Luo, C.; Lussier, M.; Mao, R.; Menard, P.; Ooi, S. L.; Revuelta, J. L.; Roberts, C. J.; Rose, M.; Ross-Macdonald, P.; Scherens, B.; Schimmack, G.; Shafer, B.; Shoemaker, D. D.; Sookhai-Mahadeo, S.; Storms, R. K.; Strathern, J. N.; Valle, G.; Voet, M.; Volckaert, G.; Wang, C.-y.; Ward, T. R.; Wilhelmy, J.; Winzeler, E. A.; Yang, Y.; Yen, G.; Youngman, E.; Yu, K.; Bussey, H.; Boeke, J. D.; Snyder, M.; Philippsen, P.; Davis, R. W.; Johnston, M. Functional profiling of the *Saccharomyces cerevisiae* genome. *Nature* **2002**, *418* (6896), 387–391.

(26) Winzeler, E. A.; Shoemaker, D. D.; Astromoff, A.; Liang, H.; Anderson, K.; Andre, B.; Bangham, R.; Benito, R.; Boeke, J. D.; Bussey, H.; Chu, A. M.; Connelly, C.; Davis, K.; Dietrich, F.; Dow, S. W.; El Bakkoury, M.; Foury, F.; Friend, S. H.; Gentelen, E.; Giaever, G.; Hegemann, J. H.; Jones, T.; Laub, M.; Liao, H.; Liebundguth, N.; Lockhart, D. J.; Lucau-Danila, A.; Lussier, M.; M'Rabet, N.; Menard, P.; Mittmann, M.; Pai, C.; Rebischung, C.; Revuelta, J. L.; Riles, L.; Roberts, C. J.; Ross-MacDonald, P.; Scherens, B.; Snyder, M.; Sookhai-Mahadeo, S.; Storms, R. K.; Veronneau, S.; Voet, M.; Volckaert, G.; Ward, T. R.; Wysocki, R.; Yen, G. S.; Yu, K.; Zimmermann, K.; Philippsen, P.; Johnston, M.; Davis, R. W. Functional Characterization of the *S. cerevisiae* Genome by Gene Deletion and Parallel Analysis. *Science* **1999**, *285* (5429), 901–906.

(27) Janke, C.; Magiera, M. M.; Rathfelder, N.; Taxis, C.; Reber, S.; Maekawa, H.; Moreno-Borchart, A.; Doenges, G.; Schwob, E.; Schiebel, E.; Knop, M. A versatile toolbox for PCR-based tagging of yeast genes: New fluorescent proteins, more markers and promoter substitution cassettes. *Yeast* **2004**, *21* (11), 947–962.

(28) Gietz, R. D.; Schiestl, R. H.; Willems, A. R.; Woods, R. A. Studies on the transformation of intact yeast cells by the LiAc/SS-DNA/PEG procedure. *Yeast* **1995**, *11* (4), 355–360.

(29) Shevchenko, A.; Wilm, M.; Vorm, O.; Mann, M. Mass spectrometric sequencing of proteins from silver-stained polyacrylamide gels. *Anal. Chem.* **1996**, *68* (5), 850–858.

(30) Gelperin, D. M.; White, M. A.; Wilkinson, M. L.; Kon, Y.; Kung, L. A.; Wise, K. J.; Lopez-Hoyo, N.; Jiang, L.; Piccirillo, S.; Yu, H.; Gerstein, M.; Dumont, M. E.; Phizicky, E. M.; Snyder, M.; Grayhack, E. J. Biochemical and genetic analysis of the yeast proteome with a movable ORF collection. *Genes Dev.* **2005**, *19* (23), 2816–2826.

(31) Mok, J.; Im, H.; Snyder, M. Global identification of protein kinase substrates by protein microarray analysis. *Nat. Protoc.* **2009**, *4* (12), 1820–1827.

(32) Christianson, T. W.; Sikorski, R. S.; Dante, M.; Shero, J. H.; Hieter, P. Multifunctional yeast high-copy-number shuttle vectors. *Gene* **1992**, *110* (1), 119–122.

(33) Xu, C.; Henry, P. A.; Setya, A.; Henry, M. F. *In vivo* analysis of nucleolar proteins modified by the yeast arginine methyltransferase Hmt1/Rmt1p. *RNA* **2003**, *9* (6), 746–59.

(34) Hart-Smith, G.; Low, J. K.; Erce, M. A.; Wilkins, M. R. Enhanced methylarginine characterization by post-translational modification-specific targeted data acquisition and electron-transfer dissociation mass spectrometry. *J. Am. Soc. Mass Spectrom.* **2012**, *23* (8), 1376–1389.

(35) Gatlin, C. L.; Kleemann, G. R.; Hays, L. G.; Link, A. J.; Yates III, J. R. Protein identification at the low femtomole level from silver-stained gels using a new fritless electrospray interface for liquid chromatography–microspray and nanospray mass spectrometry. *Anal. Biochem.* **1998**, *263* (1), 93–101.

(36) Perkins, D. N.; Pappin, D. J. C.; Creasy, D. M.; Cottrell, J. S. Probability-based protein identification by searching sequence databases using mass spectrometry data. *Electrophoresis* **1999**, *20* (18), 3551–3567.

(37) Snijders, A.; Hung, M.-L.; Wilson, S.; Dickman, M. Analysis of arginine and lysine methylation utilizing peptide separations at neutral pH and electron transfer dissociation mass spectrometry. *J. Am. Soc. Mass Spectrom.* **2010**, *21* (1), 88–96.

(38) Cherry, J. M.; Hong, E. L.; Amundsen, C.; Balakrishnan, R.; Binkley, G.; Chan, E. T.; Christie, K. R.; Costanzo, M. C.; Dwight, S. S.; Engel, S. R.; Fisk, D. G.; Hirschman, J. E.; Hitz, B. C.; Karra, K.; Krieger, C. J.; Miyasato, S. R.; Nash, R. S.; Park, J.; Skrzypek, M. S.; Simison, M.; Wong, S.; Wong, E. D. *Saccharomyces* genome database: The genomics resource of budding yeast. *Nucleic Acids Res.* **2012**, *40* (D1), D700–D705.

(39) Consortium, T. U. Reorganizing the protein space at the Universal Protein Resource (UniProt). *Nucleic Acids Res.* **2012**, *40* (D1), D71–D75.

(40) Huh, W.-K.; Falvo, J. V.; Gerke, L. C.; Carroll, A. S.; Howson, R. W.; Weissman, J. S.; O'Shea, E. K. Global analysis of protein localization in budding yeast. *Nature* **2003**, *425* (6959), 686–691.

(41) Woolderchak, W. L.; Zang, T.; Zhou, Z. S.; Acuna, M.; Tahara, S. M.; Hevel, J. M. Substrate profiling of PRMT1 reveals amino acid sequences that extend beyond the “RGG” paradigm. *Biochemistry* **2008**, *47* (36), 9456–66.

(42) Pang, C.; Gasteiger, E.; Wilkins, M. Identification of arginine- and lysine-methylation in the proteome of *Saccharomyces cerevisiae* and its functional implications. *BMC Genomics* **2010**, *11* (1), 92.

(43) Smith, J. J.; Rücknagel, K. P.; Schierhorn, A.; Tang, J.; Nemeth, A.; Linder, M.; Herschman, H. R.; Wahle, E. Unusual sites of arginine methylation in poly(A)-binding protein II and *in vitro* methylation by protein arginine methyltransferases PRMT1 and PRMT3. *J. Biol. Chem.* **1999**, *274* (19), 13229–13234.

(44) Huang, D.; Sherman, B.; Ra, L. Bioinformatics enrichment tools: Paths toward the comprehensive functional analysis of large gene lists. *Nucleic Acids Res.* **2009**, *37* (1), 1–13.

(45) Green, D. M.; Marfatia, K. A.; Crafton, E. B.; Zhang, X.; Cheng, X.; Corbett, A. H. Nab2p is required for poly(A) RNA export in *Saccharomyces cerevisiae* and is regulated by arginine methylation via Hmt1p. *J. Biol. Chem.* **2002**, *277* (10), 7752–60.

(46) Shen, E. C.; Henry, M. F.; Weiss, V. H.; Valentini, S. R.; Silver, P. A.; Lee, M. S. Arginine methylation facilitates the nuclear export of hnRNP proteins. *Genes Dev.* **1998**, *12* (5), 679–91.

(47) Xu, C.; Henry, M. F. Nuclear export of hnRNP Hrp1p and nuclear export of hnRNP Npl3p are linked and influenced by the methylation state of Npl3p. *Mol. Cell. Biol.* **2004**, *24* (24), 10742–10756.

(48) McBride, A. E.; Cook, J. T.; Stemmler, E. A.; Rutledge, K. L.; McGrath, K. A.; Rubens, J. A. Arginine methylation of yeast mRNA-binding protein Npl3 directly affects its function, nuclear export, and intranuclear protein interactions. *J. Biol. Chem.* **2005**, *280* (35), 30888–30898.

(49) Ho, E.; Webber, R.; Wilkins, M. R. Interactive three-dimensional visualization and contextual analysis of protein interaction networks. *J. Proteome Res.* **2008**, *7* (1), 104–112.

(50) Rouillon, A.; Surdin-Kerjan, Y.; Thomas, D. Transport of sulfonium compounds. Characterization of the *s*-adenosylmethionine and *S*-methylmethionine permeases from the yeast *Saccharomyces cerevisiae*. *J. Biol. Chem.* **1999**, *274* (40), 28096–28105.

- (51) Najbauer, J.; Aswad, D. W. Diversity of methyl acceptor proteins in rat pheochromocytoma (PC12) cells revealed after treatment with adenosine dialdehyde. *J. Biol. Chem.* **1990**, 265 (21), 12717–21.
- (52) Fisk, J. C.; Li, J.; Wang, H.; Aletta, J. M.; Qu, J.; Read, L. K. Proteomic analysis reveals diverse classes of arginine methylproteins in mitochondria of trypanosomes. *Mol. Cell. Proteomics* **2012**, 12, 302–311.
- (53) Rho, J.; Choi, S.; Seong, Y. R.; Choi, J.; Im, D.-S. The arginine-1493 residue in QRRGRTGR1493G Motif IV of the hepatitis C virus NS3 helicase domain is essential for NS3 protein methylation by the protein arginine methyltransferase 1. *J. Virol.* **2001**, 75 (17), 8031–8044.
- (54) Smith, W. A.; Schurter, B. T.; Wong-Staal, F.; David, M. Arginine methylation of RNA Helicase A determines its subcellular localization. *J. Biol. Chem.* **2004**, 279 (22), 22795–22798.
- (55) Lee, J.; Bedford, M. T. PABP1 identified as an arginine methyltransferase substrate using high-density protein arrays. *EMBO Rep.* **2002**, 3 (3), 268–273.
- (56) Miranda, T. B.; Sayegh, J.; Frankel, A.; Katz, J. E.; Miranda, M.; Clarke, S. Yeast Hsl7 (histone synthetic lethal 7) catalyses the *in vitro* formation of  $\omega$ -NG-monomethylarginine in calf thymus histone H2A. *Biochem. J.* **2006**, 395 (3), 563–570.
- (57) Sayegh, J.; Clarke, S. G. Hsl7 is a substrate-specific type II protein arginine methyltransferase in yeast. *Biochem. Biophys. Res. Commun.* **2008**, 372 (4), 811–815.
- (58) Costanzo, M.; Baryshnikova, A.; Bellay, J.; Kim, Y.; Spear, E. D.; Sevier, C. S.; Ding, H.; Koh, J. L. Y.; Toufighi, K.; Mostafavi, S.; Prinz, J.; St. Onge, R. P.; VanderSluis, B.; Makhnevych, T.; Vizeacoumar, F. J.; Alizadeh, S.; Bahr, S.; Brost, R. L.; Chen, Y.; Cokol, M.; Deshpande, R.; Li, Z.; Lin, Z.-Y.; Liang, W.; Marback, M.; Paw, J.; San Luis, B.-J.; Shuteriqi, E.; Tong, A. H. Y.; van Dyk, N.; Wallace, I. M.; Whitney, J. A.; Weirauch, M. T.; Zhong, G.; Zhu, H.; Houry, W. A.; Brudno, M.; Ragibizadeh, S.; Papp, B.; Pál, C.; Roth, F. P.; Giaever, G.; Nislow, C.; Troyanskaya, O. G.; Bussey, H.; Bader, G. D.; Gingras, A.-C.; Morris, Q. D.; Kim, P. M.; Kaiser, C. A.; Myers, C. L.; Andrews, B. J.; Boone, C. The genetic landscape of a cell. *Science* **2010**, 327 (5964), 425–431.
- (59) Kirmizis, A.; Santos-Rosa, H.; Penkett, C. J.; Singer, M. A.; Vermeulen, M.; Mann, M.; Bahler, J.; Green, R. D.; Kouzarides, T. Arginine methylation at histone H3R2 controls deposition of H3K4 trimethylation. *Nature* **2007**, 449 (7164), 928–932.
- (60) Samel, A.; Cuomo, A.; Bonaldi, T.; Ehrenhofer-Murray, A. E. Methylation of CenH3 arginine 37 regulates kinetochore integrity and chromosome segregation. *Proc. Natl. Acad. Sci. U.S.A.* **2012**, 109 (23), 9029–34.
- (61) Krause, C. D.; Yang, Z.-H.; Kim, Y.-S.; Lee, J.-H.; Cook, J. R.; Pestka, S. Protein arginine methyltransferases: Evolution and assessment of their pharmacological and therapeutic potential. *Pharmacol. Ther.* **2007**, 113 (1), 50–87.